ACCSCIENCE PUBLISHING

Materials Science in Additive Manufacturing

REVIEW ARTICLE

Recent progress on materials for functional additive manufacturing

Hayeol Kim[1], Kyung-Hwan Kim[1], Jiyun Jeong[1], Yunsoo Lee[1], and Im Doo Jung[1,2]*

[1]Department of Mechanical Engineering, Faculty of Mechanical Engineering, Ulsan National Institute of Science and Technology, Ulsan, Republic of Korea

[2]Artificial Intelligence Graduate School, Ulsan National Institute of Science and Technology, Ulsan, Republic of Korea

Abstract

Material science in additive manufacturing (AM) has experienced remarkable advancements in the development of functional materials. This review systematically investigates the state-of-the-art research on AM of functional materials, providing a comprehensive overview of AM systems and methodologies employed for functional materials and applications. The review delves into various functional materials, including magnetic, metal powder, perovskite, piezoelectric, thermoelectric, and carbon-based materials, exploring their fabrication and applications in creating multifunctional components and devices. Furthermore, it examines the integration of these functional materials, enabling manufacturing on curved surfaces, the development of flexible components, and the enhancement of functional properties. By analyzing the latest developments in this rapidly evolving field, this review offers insights into current challenges, future directions, and potential innovations, promoting a deeper understanding of AM technology and stimulating further advancements toward the realization of advanced functional devices and systems.

Keywords: Additive manufacturing; Functional materials; Polymer matrices; Multifunctional components

***Corresponding author:**
Im Doo Jung
(idjung@unist.ac.kr)

Citation: Kim H, Kim KH, Jeong J, Lee Y, Jung IM. Recent progress on materials for functional additive manufacturing. *Mater Sci Add Manuf*. 2024;3(2):3323. doi: 10.36922/msam.3323

Received: March 29, 2024

Accepted: May 16, 2024

Published Online: June 27, 2024

1. Introduction

Additive manufacturing (AM), commonly referred to as three-dimensional (3D) printing, manufactures objects layer by layer. This process has revolutionized the manufacturing landscape by offering enhanced design flexibility and reduced production times. AM technology enables the fabrication of complex structures and allows for the manufacturing of creative and innovative designs.[1-3] It facilitates the customized production of each product, which offers significant advantages in prototype development and personalized product manufacturing.[4,5] Moreover, AM enables the fabrication of complex structures, contributing to light weighting and structural optimization in industries such as aerospace and automotive.[6-11] With these diverse arrays of advantages, AM technology is driving innovative changes in the manufacturing industry.

Polymer materials are widely utilized in AM due to their inherent advantages, such as lightweight, corrosion resistance, mechanical strength, and biocompatibility.[4]

These polymers, ranging from photo-curable resins to thermoplastics and viscous polymer inks, find applications across diverse areas, including medical, aerospace, automotive, electronics, soft robotics, energy, environmental, and industrial fields, depending on their specific characteristics.[12,13] Moreover, recent research is exploring the potential of polymers for 4D printing, where they can respond to stimuli such as temperature, light, electric fields, magnetic fields, and moisture, resulting in changes in shape or properties over time.[14,15] The versatility and adaptability of polymer materials render them highly desirable for AM, especially when integrated with functional materials to enable a wide range of applications.

AM using functional materials has emerged as a critical area of research in the manufacturing industry. The use of polymer-based functional materials in AM offers significant advantages due to ease of processing and low manufacturing temperatures. By combining various functional materials with polymer matrices, it becomes possible to enhance the characteristics and functionalities of polymers, facilitating the fabrication of components with properties such as magnetic, actuating, and electrical conductivity.[4] Furthermore, ongoing research is exploring the fabrication of parts with properties such as piezoelectric and thermoelectric behavior by leveraging multi-material manufacturing capabilities.[16,17] The development of AM technology using functional and high-performance materials unlocks diverse applications across various industries, ranging from electronics engineering to medical purposes such as artificial organs and medical robotics.[18,19] These research efforts underscore the innovative advancements driven by AM with functional materials in the manufacturing industry and are expected to contribute to enhancing manufacturing process efficiency and product performance.

This review aims to comprehensively investigate state-of-the-art research efforts on AM of functional materials integrated with polymer matrices. It systematically categorizes AM systems and methodologies used for polymer-based functional materials. Subsequently, it summarizes notable studies that fabricate various functional materials or structures, such as magnetic, metal powder, perovskite, piezoelectric, and thermoelectric materials, exploring their applications in fabricating multifunctional components and devices. Ultimately, by studying and analyzing the latest developments in polymer-based AM of functional materials, this review seeks to provide insights into current challenges, future directions, and potential innovations in the rapidly growing field of functional AM. Figure 1 provides an overview of functional materials for AM techniques and applications. Descriptions of key strategies, material selections, and application prospects are provided to foster a deeper understanding of AM technology and stimulate further innovation toward the realization of advanced functional devices and systems.

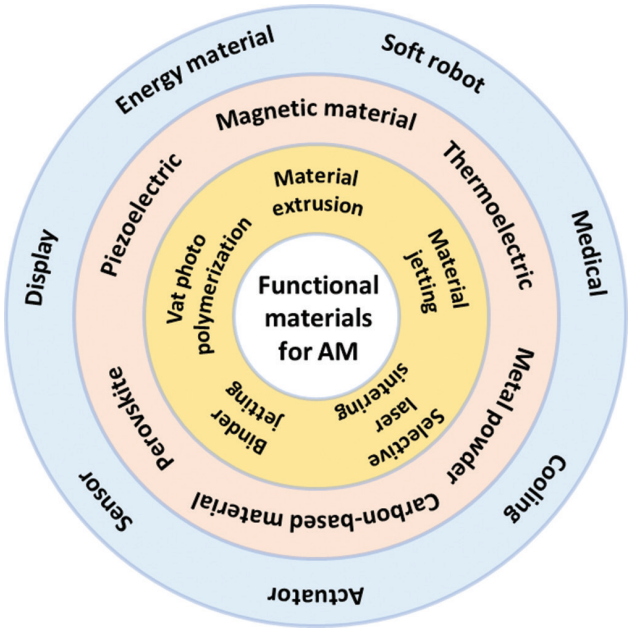

Figure 1. Overview of functional materials for additive manufacturing techniques and applications.

2. AM methods for functional materials

According to American Society for Testing and Materials standards, the AM of functional polymer materials can be classified into several categories: material extrusion, vat photopolymerization, binder jetting, powder bed fusion (PBF), and material jetting. Each AM technology has its unique manufacturing process and compatible materials, with the suitable technology varying depending on the required functional characteristics and polymer types. These classifications and characteristics are summarized in Table 1.

2.1. Material extrusion

Material extrusion is currently the most commonly used AM method, forming layers by extruding thermoplastic or liquid-state materials through small nozzles.[20] While this method may have relatively lower resolution and accuracy, its affordability and ability to mix with various materials make it widely utilized, especially in the manufacturing of functional polymers. An example of a material extrusion AM method commonly used for polymers is depicted in Figure 2A.

Fused deposition modeling (FDM) is a 3D printing technique in which molten thermoplastic material is

Table 1. Characteristics of each polymer AM process

AM process	Printing method	Raw materials	Fabrication mechanism	Resolution (xy [μm])	Resolution (thickness [μm])	Typical build size (mm^3)
Material extrusion	FDM	Thermoplastic filaments or pellets	Molten material extrusion	100 – 150	100 – 200	223×223×305
	DIW	Viscoelastic ink	Material extrusion and solidification	100 – 1200	100 – 400	260×220×70
	Meniscus printing	Viscous ink	Ink extrusion by meniscus contact	0.05 – 2	-	4×25
Vat photopolymerization	SLA	Photosensitive polymer resin	UV laser curing	6.5 – 25	25 – 300	145×145×175
	DLP	Photosensitive polymer resin	DLP projector curing	35 – 100	25 – 150	140×79×100
	CLIP	Photosensitive polymer resin	Continuous UV curing	75	0.4 – 100	150×80×300
Binder jetting	-	Powdered materials	Drop bonding liquid	100	260 – 380	1800×1000×700
Powder bed fusion	SLS	Polymer powder	Laser sintering	30 – 100	60 – 180	340×340×600
Material jetting	Polyjet	Thermoset photopolymers	Liquid material deposit and UV curing	42 – 85	16 – 28	294×192×148.6

Abbreviations: AM: Additive manufacturing; CLIP: Continuous liquid interface production; DIW: Direct ink writing; DLP: Digital light processing; FDM: Fused deposition modeling; SLA: Stereolithography; SLS: Selective laser sintering.

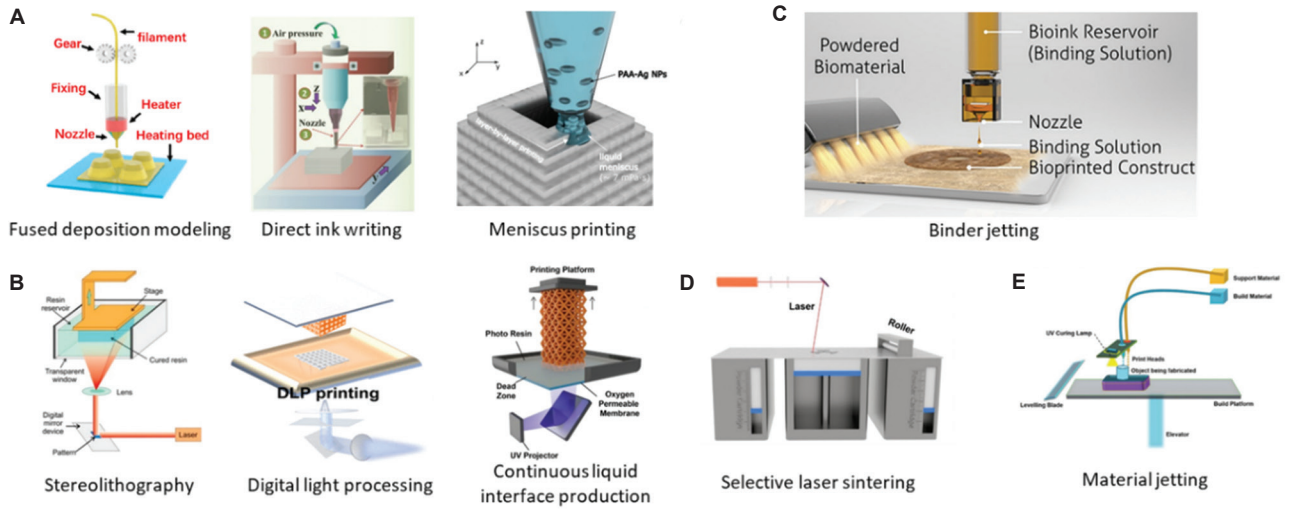

Figure 2. Schematic illustrations of the additive manufacturing process for functional materials. (A) Material extrusion 3D printing; left panel reproduced with permission from Liu *et al.*[16] (Copyright © 2022 American Chemical Society); center panel reproduced with permission from Hossain *et al.*[21] (Copyright © 2022 American Chemical Society); right panel reproduced with permission from Lee *et al.*[23] (Copyright © 2017 American Chemical Society). (B) Vat photopolymerization 3D printing; left panel reproduced with permission from Pagac *et al.*[25] (Copyright © 2018 American Chemical Society); center panel reproduced with permission from Chiappone *et al.*[27] (Copyright © 2021 American Chemical Society); and right panel reproduced with permission from Wang *et al.*[28] (Copyright © 2023 American Chemical Society). (C) Binder jetting; reproduced with permission from Jose *et al.*[29] (Copyright © 2016 American Chemical Society). (D) Selective laser sintering; reproduced with permission from Ouyang *et al.*[30] (Copyright © 2022 American Chemical Society). (E) Material jetting; reproduced with permission from Sireesha *et al.*[31] (Copyright © 2018 RSC Advances).

extruded through a movable nozzle controlled by software to create layers.[16] This process typically involves heating the thermoplastic filament to its melting point within the printer's extruder assembly. The melted filament is then precisely deposited onto the build platform layer by layer, where it quickly solidifies to form the desired object. The movement of the nozzle is directed by computer-aided design software, allowing for the production of intricate and precise shapes. Recent advancements include screw-based systems capable of using pellets, enabling the processing of a wider range of thermoplastic materials in large sizes. This expansion of capabilities has increased the scope of FDM applications in both research and industry.

Direct ink writing (DIW) is a 3D printing technique that enables the precise deposition of liquid-state materials

through small nozzles to create desired shapes. This process involves the extrusion of material in a continuous stream rather than layer-by-layer deposition typical of other 3D printing methods. DIW allows for the use of various materials, including non-thermoplastic polymers, hydrogels, ceramics, and even living cells, in bio-printing applications. The ability to print with liquid materials provides flexibility in material composition and properties, making DIW suitable for a wide range of applications in fields such as biomedicine, soft robotics, and electronics.[21,22]

Meniscus printing is a 3D printing technology wherein liquid polymers are dispensed onto a flat surface and shaped using surface tension to achieve the desired form. This method typically involves the controlled deposition of droplets of liquid polymer onto a substrate. The surface tension of the liquid causes it to form a meniscus, which can be controlled to create precise shapes and structures.[23,24] Meniscus printing offers advantages in producing complex geometries and structures with high resolution and precision. It finds applications in various fields, including biomedicine, where it can be used to create biomaterials for tissue engineering and drug delivery systems.

2.2. Vat photopolymerization

Vat photopolymerization is an AM technology that selectively solidifies liquid resin contained in a vat using a curing device. The liquid resin typically consists of oligomers and monomers. When exposed to the curing light, the oligomers and monomers undergo polymerization, forming polymer chains that harden to create the desired object. The curing process occurs layer by layer, with each layer solidified before the next layer is added, resulting in precise and detailed models. Vat photopolymerization utilizes various curing devices such as UV beams, digital light, and light-emitting diodes (LEDs), offering advantages in high resolution and accuracy for the resulting products.[25]

Stereolithography (SLA) is a high-resolution AM technology that employs rastering lasers to photopolymerize liquid resin, forming 3D models. The process involves sequentially exposing the resin surface to the laser to create layers, with each layer cured by UV light.[26] A schematic diagram of the SLA process is illustrated on the left in Figure 2B. SLA is capable of producing intricate and complex models with high precision. It finds extensive applications in industries such as advanced medical, automotive, and aerospace due to its ability to fabricate precise and complex prototypes and functional parts.

Digital light processing (DLP) stands out in the realm of AM as a technology that precisely photopolymerizes liquid resin using a projector light source. Its significant difference from SLA lies in the light source. While SLA employs rastering lasers, DLP utilizes a projector light source, enabling a different approach to layer creation. A defining advantage of DLP is its capability to print an entire 2D layer simultaneously, thanks to the digital micro-mirror device generating a digital image to illuminate each layer's shape in one go.[27] This simultaneous curing process contributes to the rapid production of high-resolution models, distinguishing DLP for its speed in manufacturing. This speed advantage positions DLP as a viable choice for applications where time-to-market is crucial, such as precision parts manufacturing and medical modeling. However, it is worth noting that compared to SLA, DLP may exhibit slightly lower resolution due to the nature of its projection method. Despite this minor drawback, DLP's efficiency in printing speed makes it an attractive option for various industries seeking to balance between speed and resolution in their AM processes.

Continuous liquid interface production (CLIP) 3D printing is an AM technology that addresses the slow production speed of SLA and DLP by fundamentally changing the manufacturing process. Instead of layer-by-layer manufacturing using photo-curable resin, CLIP continuously lowers a liquid resin pool to manufacture objects.[28] This continuous process offers significantly faster production speeds, up to 100 times faster than conventional layer-by-layer methods, while maintaining high accuracy. CLIP holds promise for manufacturing innovation due to its speed and precision, opening up new possibilities for various industries. The primary distinction between DLP and CLIP lies in their manufacturing processes: CLIP utilizes a continuous manufacturing process, whereas DLP employs a layer-by-layer approach, as illustrated in Figure 2B.

2.3. Binder jetting

Binder jetting is an AM process that begins by evenly spreading powder material across a build platform. Subsequently, a binder, typically in liquid form, is precisely jetted onto the powder layer, selectively solidifying it. This process is repeated for each layer until the desired object is formed. The schematic of the binder jetting process is depicted in Figure 2C. Post-processing techniques such as sintering or infiltrating can, further, enhance the precision and strength of the final product. Binder jetting is known for its relatively high production speeds and cost-effectiveness, making it suitable for mass production. In addition, its ability to mix various materials provides versatility for manufacturing functional components across different industries.[26]

2.4. PBF

Polymer materials are primarily utilized in the PBF process, predominantly through selective laser sintering (SLS).

SLS involves laying down a flat layer of polymer powder particles and selectively sintering them with a laser into the desired shape. After each layer is sintered, the powder bed is lowered, and another flat powder layer is laid on top, repeating the process until the entire object is fabricated. It is important to note that SLS differs distinctly from selective laser melting (SLM), as SLS does not fully melt the powder into a liquid state. The schematic of the SLS process is shown in Figure 2D. SLS technology offers the capability to manufacture complex 3D shapes, enabling its application across a wide range of fields. In addition, its ability to mix various materials further extends its versatility.[30] Particularly, noteworthy is the role of polymer powder in serving as support, enhancing design flexibility. From prototype fabrication to final product manufacturing, SLS emerges as a promising manufacturing method extensively used across diverse industries.

2.5. Material jetting

Material jetting is a manufacturing method where liquid materials are precisely sprayed through small nozzles to form layers. This technology offers exceptional fabrication speed, making it suitable for various industries and applications.[31] In material jetting, materials are deposited at precise locations through small nozzles and then cured either by UV light or heat to form and bond layers. The referenced process schematic is shown in Figure 2E. This process allows for the creation of models with complex shapes and intricate details, providing high material selectivity and enabling the fabrication of parts with specific material properties tailored to the application's requirements.

3. AM with functional materials and their applications

3.1. Magnetic powders

Recently, there has been active research on magnetically responsive soft materials among various types of polymer-based stimuli-responsive soft materials. This interest primarily stems from their advantage of faster response compared to other operating modes, such as heat, light, and electric fields.[32] The magnetic field, which serves as the actuating source for these magnetically responsive soft materials, is non-contact and relatively easy to control, as its magnitude, phase, and frequency can be modulated quickly and accurately, and the magnetic field is transparent to most materials.[32-34]

Magnetic filler particles generally consist of ferromagnetic materials that exhibit significant magnetization under an external magnetic field. These ferromagnetic materials can be classified according to their magnetization properties into hard magnetic materials, soft magnetic materials, and superparamagnetic materials. Hard magnetic materials have high remanence and coercivity. Remanence (or residual magnetization) refers to the magnetization remaining in a material after the external magnetic field has been removed. This property renders hard magnetic materials to be considered permanent magnets. Coercivity is the strength of the external magnetic field required to demagnetize the magnetized material. Hard magnetic materials can maintain significant residual magnetization even after the removal of the magnetic field following saturation, and they can also retain notable residual magnetization when subjected to magnetic fields below their coercive strength.[35,36] Due to these characteristics, hard magnetic materials exhibit large hysteresis (Figure 3A). Hence, composites containing hard magnetic particles embedded in a polymer matrix retain high residual properties after magnetization and exhibit independent behavior in response to applied magnetic fields below the coercive fields. Hard magnetic materials include ferrite-based substances such as barium ferrite ($BaFe_{12}O_{19}$), strontium ferrite ($SrFe_{12}O_{19}$), or neodymium iron boron ($Nd_2Fe_{14}B$) and samarium cobalt ($SmCo_5$, Sm_2Co_{17}) known as rare-earth magnets.

Soft magnetic materials, such as pure iron (Fe), nickel-iron alloy, and silicon-iron alloy, are known for their strong response to magnetic fields, characterized by high saturation magnetization. However, they tend to retain a low residual magnetization after saturation and are easily demagnetized due to their low coercivity. That is, soft magnetic materials have narrow hysteresis (Figure 3B). In addition, these materials, utilized as fillers, possess high relative permeability and swift responsiveness, making them widely utilized in the fabrication of magnetic alignment composites.[35] Ferromagnetic particles smaller than a certain critical size are referred to as superparamagnetic materials, behaving somewhat similarly to non-magnetic substances in the absence of an external magnetic field, despite maintaining relatively high magnetization (Figure 3C). Superparamagnetism is a property exhibited by nanometer-sized magnetic particles, where the continual thermal motion and Brownian motion cause their magnetic structure to fluctuate, rendering them essentially unaligned in the absence of an external magnetic field. Notably, Fe_3O_4 nanoparticles are widely utilized in various fields, including biomedical applications and micro-robotics, due to their biocompatibility and relatively high magnetization.[37-39] Typically, Fe_3O_4 undergoes a transition from a soft magnetic phase to a superparamagnetic phase at a critical size of around 20 nm.[40]

3.1.1. Magnetically responsive soft robots

Due to recent advances in 3D printing technology for soft materials, current research is focused on developing soft

robots capable of achieving complex behaviors through the use of 3D-printed magnetically responsive soft materials (Table 2). Embedded magnetic filler particles generate internal stress as they attempt to align with the magnetic field under external magnetic influence, resulting in macroscopic deformation and exhibiting intricate behavior.[41-43]

A method has been developed to program complex non-uniform magnetic domain patterns using permanent magnets or electromagnets on hard magnetic particles

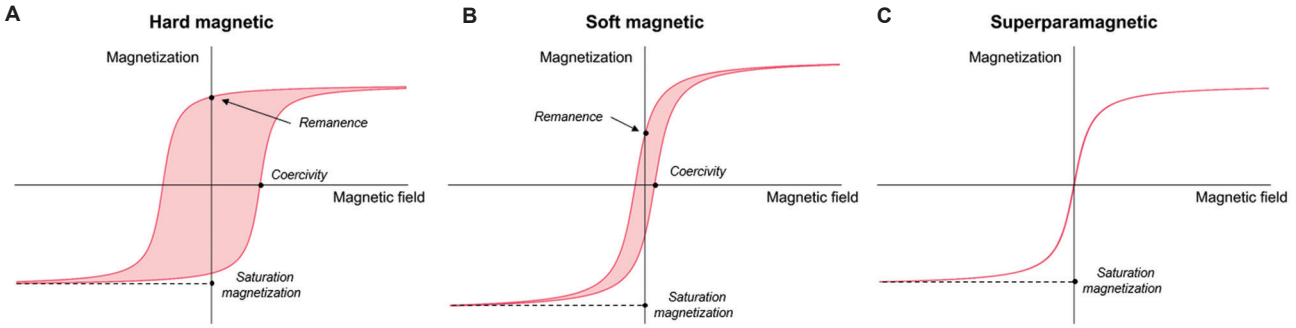

Figure 3. Comparison of magnetization characteristics under magnetic field. (A) Hard magnetic materials. (B) Soft magnetic materials. (C) Superparamagnetic materials.

Table 2. Comparison of materials and fabrication methods for magnetically responsive soft robots

3D printing method	Material composition	Description	References
Material extrusion (DIW)	NdFeB microparticles+thermoplastic elastomers (styrene-isoprene block copolymers)	NdFeB-SIS composite ink is developed to provide high elasticity (>1000%), and an origami-inspired printing method is introduced for reprogramming.	41
Material extrusion (DIW)	NdFeB microparticles+silicone elastomers (SE1700 and Ecoflex 00-30 Part B)	The evolutionary algorithm-guided voxel encoding is proposed to design tailored magnetic density and direction, leading to functional biomimetic soft robots and expanded applications.	42
Material extrusion (DIW)	NdFeB microparticles+silicone elastomers (SE1700 and Ecoflex 00-30 Part B)	A new 3D printing technology is proposed for shape-programmable soft materials utilizing magnetic fields for untethered actuation and delivering potential for biomedical devices, and soft robotics via customized domain patterns and magnetization strength.	44
Material extrusion (DIW)	NdFeB microparticles+silicone elastomers (Sylgard 184)	A 4D printing method utilizing an origami-based magnetization technique is proposed. This method enables the fabrication of complex objects with the ability to reprogram their magnetization. Bionic hands serve as an example of this capability.	43
Material extrusion (DIW)	NdFeB microparticles+thermoplastic elastomers (thermoplastic urethane) NdFeB microparticles+silicone elastomers (Sylgard 184)	A continuum soft robot with omnidirectional steering capabilities, miniaturized ferromagnetic domains, and hydrogel skin for navigation in complex environments and steerable laser delivery was presented for minimally invasive robotics surgery.	45
Material extrusion (DIW)	NdFeB microparticles+silicone elastomers (SE 1700)	A coaxial printing method for creating soft-magnetic-electrical fibers is presented, enabling hybrid functions issues in soft robotics and biomedical applications, demonstrated by catheter-based electro-ablation, somatosensory gripper.	47
Vat photopolymerization (DLP)	NdFeB microparticles+photocurable elastomers	A UV lithography-based method is presented for patterning magnetic particles in elastomer matrices, enabling custom 3D magnetization profiles for higher-order microrobots, leading to locomotion with multi-arm grasping and multi-legged crawling.	49
Vat photopolymerization (CLIP)	Fe_3O_4 nanoparticles+photocurable elastomers	A comprehensive solution for designing and fabricating a 3D micro-robotic gripper using a high-resolution CLIP process for untethered operation in both dry and aqueous environments has been presented, resulting in a monolithic gripper design.	50

Abbreviations: CLIP: Continuous liquid interface production; DIW: Direct ink writing; DLP: Digital light processing; NdFeB: Neodymium magnet.

inside soft materials utilized in extrusion-based 3D printing, such as DIW.[44] Soft materials embedded with neodymium magnet (NdFeB) particles, programmed through this method, can undergo rapid transformations of complex shapes under the influence of an external magnetic field. Building on this capability, a soft robot capable of crawling and jumping was developed. Similarly, a method has been developed that can program not only the direction but also the density of the magnetic domain on a voxel basis in the printed filament using an evolutionary algorithm.[42] Through this approach, a four-legged soft robot mimicking a trot (dog gaits) was developed from a soft material embedded with NdFeB particles under an alternating magnetic field. This demonstration highlights the potential for greatly expanding application possibilities beyond the brute-force approach used to program the magnetization domain of existing magnetically responsive soft materials.

A mechanism was proposed to reprogram the magnetization profile by folding a hinge-designed magnetically responsive material into a desired shape and applying an impulse magnetic field exceeding the coercivity. Using this mechanism, a multi-finger soft robotic gripper exhibiting precise operation was demonstrated (Figure 4A).[41] A rock-paper-scissors gesture was demonstrated by re-magnetizing a magnetically responsive NdFeB material that mimics the human hand.[45] For hard magnetic materials that are already saturated, the remanence can be initialized by heating and cooling above the Curie point of the material in addition to applying an impulse magnetic field greater than the coercive force.

The self-responsive soft material is soft and flexible while exhibiting excellent responsiveness, enabling expansion into a core-sheath structure through integration with a functional core. Several studies have explored its application in biomedical contexts. For instance, a soft robotic catheter was developed using a polymer matrix embedded with NdFeB particles as a sheath and inserting other functional materials coaxially into the core.[46] This catheter robot, featuring an optical fiber as its functional core and a magnetically responsive soft material coated with hydrogel as its sheath, demonstrated laser delivery by reaching the target point within a 3D cerebrovascular phantom through flexible motion. Similarly, a coaxial printing method has been developed, enabling the simultaneous printing of the core and sheath to yield structures with excellent magnetic reactivity and conductivity. This method involves using a conductive liquid metal core and a magnetically responsive soft material sheath structure embedded with NdFeB particles.[47] Employing this coaxial printing method, a soft robot gripper has been developed, capable of grabing objects of various sizes by transforming under the influence of a magnetic field. In addition, a soft robot gripper capable of detecting the size of the captured object by analyzing the changing induced magnetic field was demonstrated.

In addition to extrusion-based 3D printing methods, the design and fabrication of magnetically responsive soft materials using light-based 3D printing methods have been reported. Compared to extrusion-based 3D printing, which typically has relatively lower resolution, light-based 3D printing generally has high resolution.[48] By utilizing this technology, an eight-legged paddle-crawling robot was developed by programming magnetic domains into NdFeB particles embedded within a magnetically responsive soft material.[49] Demonstrations of the robot's crawling motion on silicone oil were achieved by applying an alternating magnetic field. Furthermore, a micro-scale robotic gripper was developed using the CLIP approach instead of the slower SLA approach, which exhibits clear boundaries between layers.[50] This gripper utilizes Fe_3O_4 with a diameter of 20 – 30 nm, considered a superparamagnetic material, as a filler for achieving fast closing motion.[40] The low residual magnetization enables rapid closing of the gripper by its elasticity.

3D printing technology has revolutionized the field of magnetically responsive soft robots, enabling the creation of complex designs and sophisticated functionalities that were previously unattainable through traditional manufacturing methods. Material extrusion 3D printing offers the ability to program the magnetization direction of the printed filament by applying an external magnetic field, allowing for customized designs. This technique has proven particularly useful for fabricating soft robots with intricate structures and tailored properties. Vat photopolymerization 3D printing also provides the capability for localized magnetization programming during layer-by-layer printing. Light-based 3D printing generally offers higher resolution and faster printing speeds compared to extrusion-based methods. However, the use of dark magnetic materials can lead to reduced curing speeds, limiting the incorporation of high magnetic particle contents.

Despite the rapid advancements in 3D-printed magnetically responsive soft robots, several areas still require improvement:

(i) Real-time feedback-based autonomous control: In soft robotic applications, such as navigating through blood vessels, real-time feedback is crucial for obstacle avoidance and path planning. Vision-based feedback systems can be integrated with electromagnetic actuation systems to enable intelligent control and maneuverability.

(ii) Multi-material printing: The combination of materials with different magnetic properties using multi-nozzle printers opens up possibilities for creating

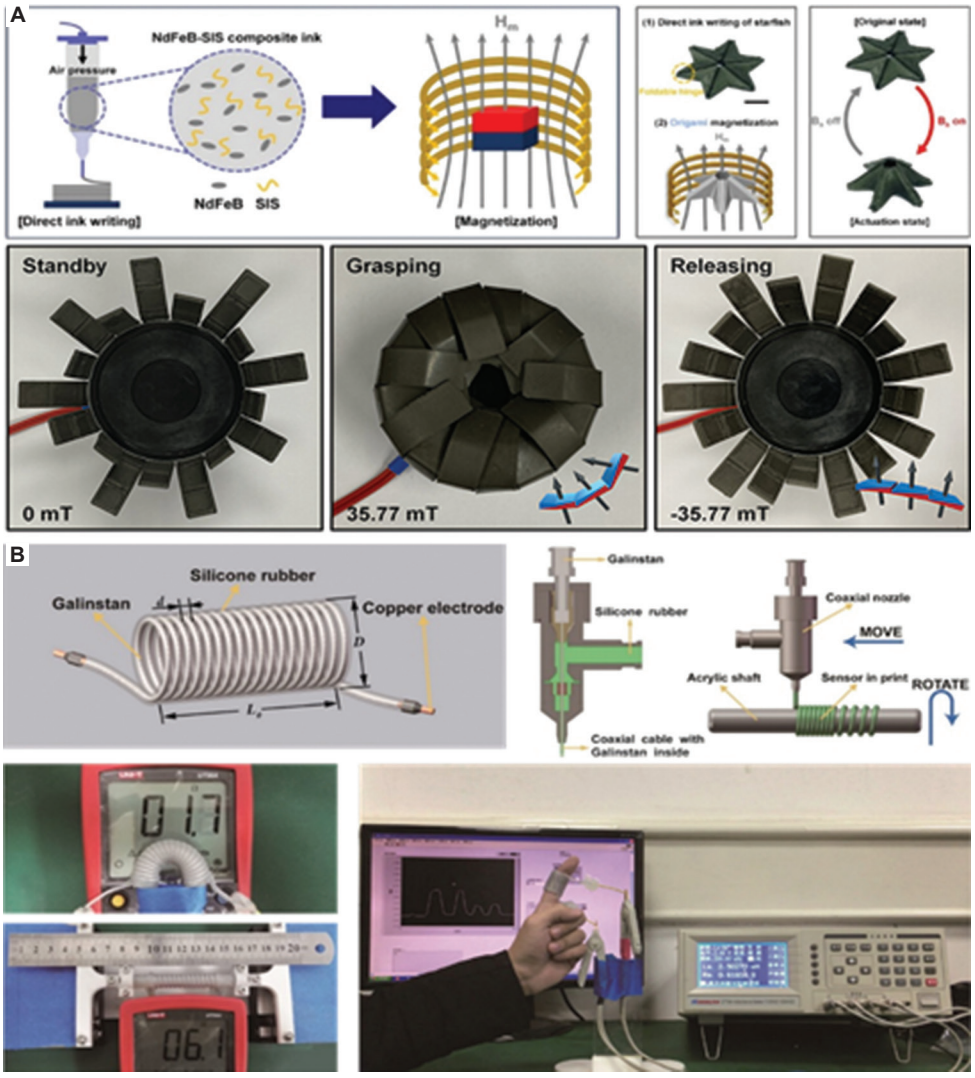

Figure 4. Polymer-based applications of magnetic powder- and metallic powder-embedded materials. (A) Origami-based programming magnetization profile method and soft robots based on magnetically responsive soft materials. Images reproduced with permission from Wajahat *et al.*[41] Copyright © 2023 American Chemical Society. (B) Soft wearable inductance sensor fabricated with a liquid metal core-polymer sheath structure. Images reproduced with permission from Zhou *et al.*[74] Copyright © 2018 American Chemical Society.

multifunctional soft robots. Integrating magnetic materials with other functional materials, such as biocompatible or conductive materials, can expand the capabilities and applications of these robots.

(iii) High magnetic particle content limitations in vat photopolymerization: While vat photopolymerization offers advantages like high resolution, it presents a challenge when using dark magnetic particles. These particles can hinder the curing process due to light absorption, making it difficult to achieve high magnetic particle content within the printed structures. This limitation can restrict the overall magnetic strength and functionality of the soft robots produced using this method.

3.2. Metal powders

In recent years, there has been remarkable progress in the field of electronic devices, especially with the emergence of soft electronics based on polymer matrices, which have seen significant advancements following the recent strides in 3D printing technology. Nanoparticle fillers can be added to polymers to impart various properties.[51] Among these, metal nanoparticle inks are readily available and exhibit relatively high electrical conductivity compared to inks containing other types of nanofillers.[52] These metal nanoparticles are used to develop a variety of flexible or stretchable soft electronics by combining embedded polymer composite ink, conformal printing,

and 3D printer technology, which allows for on-demand production.

Metal nanoparticle fillers have a direct impact on the electrical and mechanical characteristics of the printed products.[52-54] To determine the suitability of metal nanoparticles, factors such as electrical conductivity, oxidation stability, and electrical properties can be considered based on the required performance of individual soft electronics. The most commonly used metal nanoparticles are those of single elements, such as silver, gold, and copper nanoparticles.[52-56] Among them, silver is the most widely used conductive filler due to its outstanding electrical conductivity, mechanical rigidity, and high corrosion resistance among metals.[55-59] Moreover, silver nanoparticles find extensive use in medical applications, as they can be employed for selective laser photothermal treatment, leveraging the surface plasmon resonance effect and the ability to convert strongly absorbed light into local heat.[60-62] Copper nanoparticles are relatively inexpensive compared to silver and gold and possess similar electrical conductivity and a low electron transfer effect as silver.[53,54] However, when forming copper nanoparticles in air, an oxide layer is generated on the surface for thermodynamic stability, leading to a reduction in electrical conductivity and an increase in sintering temperature.[63-66] The formation of an oxide layer renders the sintering of copper nanoparticle inks technically challenging, which is one of the main reasons why copper nanoparticles are used less frequently than the relatively more expensive silver nanoparticles as conductive fillers.

3.2.1. Soft sensors embedded with metallic nanoparticles

Polymer-based sensors printed using 3D printing technology can achieve excellent shape restoration and perform various functions depending on the embedded conductive material. Particularly, polymer composites embedded with conductive nanoparticles are known to exhibit a sensitive resistance response to strain and possess excellent electrical conductivity.[67-69] An ideal elastic conductor maintains constant high conductivity over a wide range of strain rates.[70] In particular, strain and tactile sensors made of metals with excellent conductivity are actively being researched. The material, fabrication method, and performance of the polymer-based sensor embedded with metallic particles are summarized in Table 3.

Taking advantage of the fact that extrusion-based DIW 3D printing allows for multi-material printing, a tactile sensor was demonstrated through a single process with four different independently addressable nozzles.[71] The tactile sensor comprises two electrode layers, one insulating layer, a support layer, a sensor layer, and a base layer. The sensor layer and electrode layer contained silver nanoparticles embedded in silicone elastomer, and the completed sensor exhibited high flexibility, electrical conductivity, and sensitivity. It is also possible to expand it into an array form.

Strain sensors and capacitive sensors fabricated using a new method called hybrid 3D printing have been reported.[72] Advanced soft sensors are accomplished

Table 3. Comparison of materials, fabrication methods, and performance of soft sensors embedded with metallic nanoparticles

3D printing method	Material composition	Applications	Performances	References
Multi-material extrusion (DIW)	Submicrometer-sized silver particles+silicone elastomers (Dragon Skin 10)	Tactile sensor	As the pressure applied rose from 100 to 500 kPa, the device's resistance decreased approximately twelvefold, dropping from 1.14 kΩ to 95 Ω; gauge factor: about 180	71
Material extrusion (DIW) with automated pick-and-place	Silver micro-flakes+thermoplastic elastomers (thermoplastic urethane)	Microcontroller device and wearable device	Electrical conductivity; initial: 10^4×S/cm; at strain of 240%: 0.1 S/cm; gauge factor 13.3	72
Feedback-controlled material extrusion (DIW)	Silver micro-flakes+poly (ethylene oxide) (PEO)	Inductive coil (also suitable for moisture sensing), wearable device	Electrical conductivity (1.38±0.0814) × 10^4 S/cm (one order of magnitude lower than bulk silver)	73
Coaxially material extrusion (DIW)	Galinstan+silicone elastomers (737 neutral cure sealant)	Strain sensor	Maximum tensile strain of 100%; can be bent up to 180 degrees	74
Integrating vat photopolymerization (DLP) and material extrusion (DIW)	(i) DLP elastomer: acrylate-based (ii) DLP plastic: acrylate-thiol based (iii) DIW ink: photosensitive ink, conductive silver ink, and LCE ink	Strain gauge	Gauge factor: 251	75

Abbreviations: DIW: Direct ink writing; DLP: Digital light processing; LCE: Liquid crystal elastomers.

through the integration of DIW printing and automated pick-and-place of electronic components within a unified manufacturing platform. Ink using silver flakes as filler in a thermoplastic polyurethane (TPU) matrix is printed as a strain gauge, along with a pick-and-place microcontroller and LED, resulting in the development of a large-area wearable strain gauge. The developed strain gauge outputs LED readings according to joint bending. Similarly, a moisture sensor was developed through a pick-and-place hybrid procedure of DIW 3D printing and surface-mount electronic components (LEDs).[73] Polyethylene oxide (PEO) composite with silver flakes as conductive filler was extruded and printed in the form of an induction coil. When immersed in water, the printed conductive traces undergo a reverse drying process and exhibit higher impedance. Under controlled moisture, the ink maintains its printed shape and recovers to its initial impedance level after drying.

In addition, a flexible sensor was developed to detect the deformation and posture of a snake-like soft robot based on liquid metal (Figure 4B).[74] Liquid metal-based sensors have the advantage of measuring large deformations by remaining connected even after experiencing large deformations due to their stable electrical properties. Since liquid metal has low printability, silicon and liquid metal are printed together coaxially. The sensor is printed in the shape of a solenoid and can be installed on a soft robot, such as a snake, to distinguish tensile and bending deformations.

Extrusion-based 3D printing has been considered the predominant approach for fabricating soft sensors embedded with metallic powder. However, a limited but notable alternative has been reported: vat photopolymerization printing. Photopolymerization-based printing is only applicable to photosensitive resins, and metallic powders may absorb and reflect light, potentially impeding sufficient light penetration into the material. These limitations can result in incomplete curing of the material and degradation of mechanical properties. In addition, metallic powders have high thermal conductivity, which can concentrate heat energy generated during the photopolymerization process onto the soft material, leading to thermal damage or deformation of the material.

To circumvent these limitations, hybrid 3D printing that integrates the advantages of vat photopolymerization and extrusion-based 3D printing was developed. This approach has demonstrated strain gauge fabrication.[75] The hybrid 3D printer combines DLP for high-resolution printing of a photosensitive matrix and DIW for printing conductive silver nanoparticle ink. Through optimization of printing parameters, strong interfacial bonding between the DLP-printed matrix and DIW-printed functional materials was achieved. The developed strain gauge exhibited a gauge factor of 251, indicating relatively excellent sensitivity.

Advanced 3D printing techniques, such as multi-material extrusion, hybrid printing, and coaxial printing, have emerged as powerful tools for fabricating soft sensors. These 3D printing methods have particularly facilitated soft sensors embedded with metallic nanoparticles, enabling immediate fabrication on request. The integration of metal particles into non-conductive polymer matrices imparts electrical conductivity, while the inherent flexibility of polymers facilitates their applications in various fields, such as strain sensors and wearable sensors. Despite their advantages, metal particle-embedded soft materials face several challenges:

(i) High-temperature sintering: Metal nanoparticles often require high-temperature sintering (typically above 100°C) to enhance electrical conductivity, hindering *in situ* fabrication within the human body.
(ii) Cost limitations: Silver nanoparticles, the most commonly used, are expensive, thereby limiting their suitability for mass production. Although copper nanoparticles are cheaper than silver nanoparticles, they are less commonly used due to the aforementioned manufacturing difficulties.
(iii) Oxidation: The large surface area of nanoparticles makes them susceptible to oxidation, potentially compromising their long-term performance.

3.3. Perovskites

Perovskite materials have attracted considerable interest in the semiconductor field due to their unique characteristics, such as strong absorption coefficients, excellent tolerance to defects, and high charge carrier mobility.[76-78] Perovskites generally possess ABX_3 structure, where A and B represent cations, and X represents an anion (A: MA^+ or FA^+ or Cs^+, B: Pb^{2+} or Sn^{2+}, X: Cl^- or Br^- or I^-). The enhanced photoluminescence quantum yield (PLQY) and superior color purity inherent to perovskites significantly enhance the power conversion efficiency (PCE) in solar cells.[79-83] Furthermore, their broad wavelength spectrum facilitates the generation of diverse light colors in LEDs, which plays a critical role in achieving high-resolution display technologies.[84,85] Moreover, these properties are critically harnessed in engineering highly sensitive sensors capable of detecting subtle environmental alterations.[86] Conventional fabrication methods of perovskite devices include spin coating,[87] spray coating,[88] and blade coating.[89] However, spin coating often leads to substantial material loss, spray coating poses challenges in controlling the uniformity of perovskite layer thickness, and blade coating encounters difficulties in fabricating ultrathin films.

3D printing technology has emerged as an alternative that overcomes the limitations of conventional fabrication methods. It enables the fabrication of complex structures, optimization of material usage, and cost-effective production. In particular, it has been employed for fabricating perovskite layers using inkjet printing,[90] meniscus printing,[91] electrohydrodynamic (EHD) printing,[92] FDM,[93] and DIW.[94] However, securing high-quality and stable inks remains a significant challenge. Technological advancements in the fabrication and performance of perovskite materials using 3D printing technology are detailed in Table 4, highlighting their application in devices such as solar cells, sensors, and LEDs.

3.3.1. Photovoltaic effect

Perovskite solar cells (PSCs) and photodetectors both leverage the light absorption properties of perovskites to generate electrical signals from light energy. In PSCs, light induces the generation of electron-hole pairs within the active perovskite layer, which are, then, transported through the hole transport layer (HTL) and electron transport layer (ETL) to electrodes, thereby transforming light into electricity. Similarly, perovskite photodetectors generate electron-hole pairs on exposure to light, guiding them toward electrodes to produce electrical signals for detecting light intensity and wavelength. These applications are pivotal in various fields, such as environmental monitoring, image sensing, and optical communication, requiring high sensitivity and rapid response times. These technologies underscore the versatility and efficiency of perovskites in converting light into electrical energy for various practical applications.

Inkjet printing achieves a high PCE of more than 21%, replacing the conventional spin coating method due to difficulties in scaling up to large areas. This advancement was facilitated by utilizing a high-concentration precursor to effectively form absorption layers thicker than 1 μm, and by streamlining the manufacturing process through a single-ink approach.[95] Perovskite photodetectors with high resolution, flexibility, and wide color range have been fabricated using EHD printing, overcoming the limitations of fabricating multi-spectral semiconductors. This printing technique successfully produced high-quality perovskite dot arrays with 1 μm precision, presenting the potential for future wide-color photodetector and artificial vision systems.[96]

3.3.2. Perovskite displays

In perovskite LEDs and through photoluminescence in perovskites, the interplay of electrons and holes is crucial for the conversion of electrical and absorbed light energy into emitted light of various wavelengths. Electron-hole recombination within the perovskite layer is key to the efficiency of light emission in LEDs, where the introduction of various nanoparticles allows for a spectrum of colors with high purity. Photoluminescence, on the other hand, involves the absorption of photons that excite electrons to higher energy states. Following this excitation, some energy is lost, and the remaining energy is emitted as light when the

Table 4. Fabrication methods and applications using perovskite

3D printing method	Structure	Applications	Description	References
Inkjet	$Cs_{0.1}MA_{0.15}FA_{0.75}$, $Pb(I_{0.85}Br_{0.15})_3$	Solar cells	Inkjet-printed micrometer-thick perovskite solar cells achieve high power conversion efficiencies (PCEs) exceeding 21% and are promising for scalable applications in photovoltaic technologies.	95
Electrohydrodynamic (EHD)	$MAPbX_3$	Photodetector	The high-resolution perovskite full-colored photodetector achieves a responsivity of 14.97 A W^{-1}, a detectivity of 1.41×10^{12} Jones and features 1 μm diameter dot arrays.	96
Inkjet	$CsPbBr_3$	Displays (LEDs)	The inkjet-printed perovskite photodetector reported a PLQY of 61.8% and an external quantum efficiency (EQE) of 5.9%.	97
Inkjet	$FA_{0.8}Cs_{0.2}PbI_3$, $CsPbBr_3$, $Cs_{0.75}EA_{0.25}PbBr_3$	Displays (LEDs)	Perovskite light-emitting diodes (PeLEDs) exhibit a PLQY of 14.3% and are used in flexible, large-area panel lighting and displays, offering high resolution.	98
Inkjet	$CsPbBr_3$-PVP	Displays	Inkjet-printed perovskite nanocomposites achieve a 64.3% PLQY and are used for detailed, high-resolution patterning in applications like anticounterfeiting labels.	99
Meniscus	$MAPbX_3$	Displays	The meniscus-guided 3D printing technique enables the creation of perovskite nanowire heterostructures with nano-pixel resolution, facilitating innovative applications in high-resolution optoelectronics.	91

Abbreviations: PLQY: Photoluminescence quantum yield; LEDs: Light-emitting diode.

electrons return to lower energy states. This process enables perovskites to emit light at wavelengths different from the absorbed light, showcasing their potential to produce diverse and pure colors in lighting and display technologies.

LEDs were fabricated using $CsPbBr_3$ nanocrystals that maintain their crystalline structure and exhibit high PLQY even under high-temperature annealing. A novel inkjet printing technique utilizing high-boiling decalin and octane-mixed solvents was developed. This method demonstrated a six-fold increase in efficiency compared to LEDs fabricated using conventional spin coating.[97] Perovskite LEDs (PeLEDs) have garnered attention due to their characteristics, such as solution processing, large-area fabrication, and flexibility, which contrast with those of conventional inorganic LEDs. However, challenges arise when applying blade or slot-die coating to flexible substrates. In a separate study, large-area fabrication was achieved through inkjet printing technology. The fabricated PeLEDs exhibited an external quantum efficiency (EQE) of 14.3% at an area of 0.04 cm^2, suggesting the feasibility of future wide-color displays.[98]

Inkjet printing capable of precision control was implemented by adding polyvinylpyrrolidone (PVP) to perovskite. This technology is activated by light, exhibiting a fluorescent effect. The patterns created are composed of dot microarrays, exhibiting homogeneity at a macroscopic level and high reproducibility at a microscopic level. In the pertinent study, the arrangement of these dots enabled the creation of complex images such as barcodes, the logo of Fuzhou University, and honeybee illustrations. Perovskite exhibits nearly invisible characteristics in ambient conditions and can be applied to flexible substrates, indicating its potential for use in anticounterfeiting labels (Figure 5A).[99] Furthermore, complex-shaped and compositionally diverse perovskite heterostructures were fabricated using meniscus-guided printing. A study demonstrated the capability to program various emission colors, achieving color mixing and encryption at the single nanopixel level.[91]

Perovskite printing technology is garnering attention for its potential applications in flexible electronics and wearable devices due to its high material utilization efficiency and cost-effectiveness. This technology enables direct printing on flexible substrates, offering significant design flexibility and the ability to create precise patterns through fine nozzles, making it ideal for producing high-resolution displays. However, devices such as PSCs and photodetectors face challenges in maintaining long-term performance stability due to their sensitivity to environmental factors such as humidity and temperature. To overcome these challenges, further research emphasizes optimizing the chemical and physical properties of the ink, as well as exploring encapsulation and specialized coating techniques. Such advancements are expected to enhance the commercial viability of perovskite inkjet printing technology. In addition, ongoing studies focusing on optimizing ink viscosity, surface tension, and chemical properties are crucial for advancing this field.

3.4. Piezoelectrics

Piezoelectric technology possesses the capability to convert mechanical energy, such as vibrations or impacts, into electrical energy, and vice versa. The piezoelectric and converse piezoelectric effects are mathematically described by **Equations I and II**, respectively.

$$D = dT + \in^T E \quad \text{(Piezoelectric effect)} \quad \text{(I)}$$

$$S = s^E T + dE \quad \text{(Converse piezoelectric effect)} \quad \text{(II)}$$

In these equations, D represents electric displacement, d the piezoelectric charge coefficient, T mechanical stress, $\in^T$ permittivity of the material (for T = constant), E electrical field, S mechanical strain, and s^E mechanical compliance (for E = constant). The piezoelectric charge coefficient, d, varies depending on the material and its orientation, reflecting the material's effectiveness in converting mechanical energy into electrical energy and vice versa. This technology is crucial in the development of compact electronic devices, such as portable gadgets, medical technologies, and Internet of Things devices.[100,101] It enables continuous operation without the need for recharging, thereby gaining recognition as an environmentally friendly material.

Piezoelectric materials are categorized into ceramics and polymers. Ceramic materials include lead zirconate titanate (PZT)-based compounds, which possess high piezoelectric constants and ferroelectric properties,[102] as well as lead-free materials, such as $BaTiO_3$, known for their environmental friendliness.[103] On the polymer side, materials such as polyvinylidene fluoride (PVDF) and P(VDF-TrFE) are prominent, particularly in wearable technologies, due to their flexibility and ease of processing.[104,105]

Conventional manufacturing methods for piezoelectric devices, including sintering, etching, and cutting,[106-108] exhibit limitations in creating complex geometries. These methods often result in issues such as mechanical stress, loss of grain structure, reduction in strength, and near-surface depolarization.[109]

The introduction of 3D printing technology has addressed these challenges, offering advantages over traditional manufacturing methods as follows: (i) the capability to fabricate complex structures, (ii) precise

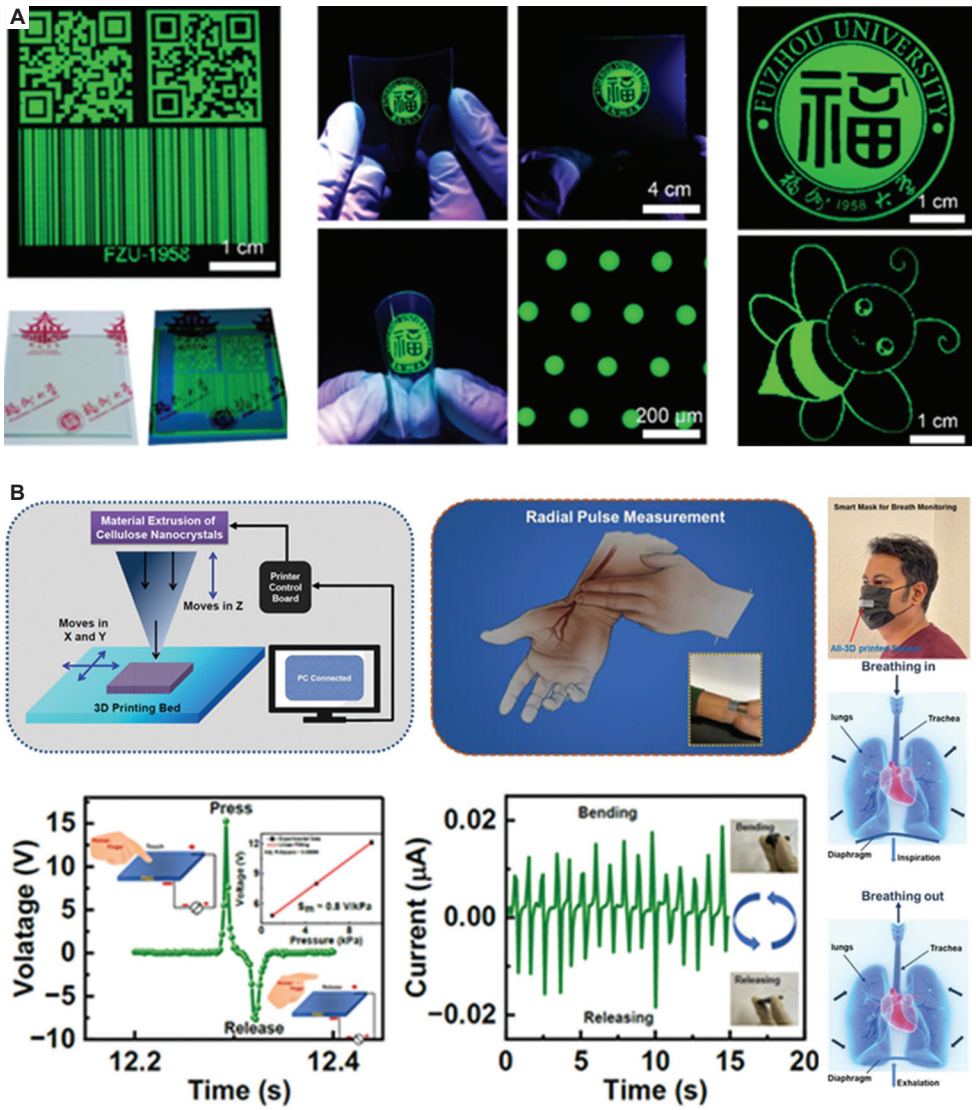

Figure 5. Applications of perovskite and piezoelectric materials. (A) Microarrays of anticounterfeiting labels made from perovskites with polyvinylpyrrolidone. Images reproduced with permission from Liu *et al.*[99] Copyright © 2019 American Chemical Society. (B) All-3D-printed pyroelectric NG (PyNG) applications, such as self-powered sensors and energy harvesting. Images reproduced with permission from Maity *et al.*[115] Copyright © 2023 American Chemical Society.

control over microscale components, (iii) simplification of device assembly and packaging stages, and (iv) enhanced electromechanical responses and piezoelectric output.[109] Piezoelectric devices are primarily manufactured using 3D printing methods such as SLA,[110] FDM,[111] DIW,[112] DLP,[113] and inkjet printing.[114] These techniques provide the potential for precise and efficient fabrication of complex 3D piezoelectric structures. Recent advances in 3D printing technology for piezoelectric materials are summarized in Table 5, highlighting their improved performance and applications in sensors, pressure detectors, and energy harvesting devices.

3.4.1. Energy harvester and sensors

Piezoelectric materials can convert mechanical stress or vibrations into electrical energy through structural deformation, leading to charge separation and accumulation. This process generates a potential difference, aiding in the transformation of mechanical to electrical energy, which can power devices immediately or be stored for future use. Widely adopted in the industrial sector for its accuracy and quick response, piezoelectric materials enable precise measurements of vibrations, pressure, and force, converting mechanical energy changes into electrical signals for application in various technologies.

Table 5. Comparison of materials and fabrication methods for piezoelectrics

3D printing method	Material composition	Applications	Description	References
FDM	Cellulose nanocrystal, CNT	Energy Harvester and sensors	An all-3D-printed pyro-piezoelectric nanogenerator using cellulose nanocrystals is introduced for self-powered cardiorespiratory monitoring, facilitating non-invasive health tracking.	115
DIW	PVDF, MoS_2	Energy Harvester and sensors	3D printing and 2D MoS2 nanofillers enhanced PVDF-based sensors, achieving a piezoelectric coefficient of 48.4 pC N^{-1}, approximately 8.2 times higher than as-cast PVDF for advanced precision applications.	116
DIW	P (VDF-TrFE), $BaTiO_3$	Sensors	A fully printed piezoelectric pressure sensor demonstrated in this work achieves a stable output of approximately 2.5 V at 30 kPa over 2000 seconds with minimal variation and is effectively employed in a prosthetic hand to discern the tactile hardness of various objects.	117
DLP	PZT, SiOC	Piezo actuators	The described multi-material additive manufacturing technique crafts intricate 3D robotic metamaterials with piezoceramic, metallic, and structural elements, enabling small-scale devices capable of complex motions and integrated sensing for advanced robotic and transducer applications.	118

Abbreviations: CNT: Carbon nanotube; DIW: Direct ink writing; DLP: Digital light processing; FDM: Fused deposition modeling; PZT: Lead zirconate titanate; PVDF: Polyvinylidene fluoride; SLA: Stereolithography; SLS: Selective laser sintering.

A hybrid thermoelectric-piezoelectric nanogenerator, utilizing cellulose nanocrystals to harvest mechanical and thermal energy, was fabricated using FDM. This 3D printing methodology reduces the number of processing steps required for multilayer fabrication while maintaining excellent stability and performance. The fabricated sensor exhibits superior mechanical energy harvesting and can accurately detect heartbeats and respiration regardless of time and location without an external power source. Furthermore, the device facilitates noninvasive monitoring of cardiorespiratory status, representing an advancement in the development of human-machine interfaces through its self-powered operation (Figure 5B).[115] Sensors fabricated using DIW with MoS_2-enhanced PVDF demonstrated a piezoelectric coefficient (d_{33}) of 48.4 pC N^{-1}, which is approximately eight times higher than that of sensors produced through casting.[116] In addition, a fully printed and PDMS-packaged piezoelectric sensor using P(VDF-TrFE)-$BaTiO_3$ was fabricated through DIW. The fabricated sensor was successfully attached to a prosthetic hand, enabling it to detect dynamic tactile data and identify objects.[117]

3.4.2. Piezo actuators

The inverse piezoelectric effect converts external electrical signals into mechanical energy, leading to the physical deformation of piezoelectric materials. When voltage is applied, the material's crystal structure deforms, slightly changing its dimensions. The extent of this expansion or contraction is influenced by the magnitude and direction of the applied voltage and the type of material. This precise control over deformation is utilized in applications such as precision positioning, vibration generation, and fluid control. These capabilities underline the significance of the inverse piezoelectric effect in various technological fields.

A robotic metamaterial utilizing DLP technology has been fabricated, featuring multi-degree-of-freedom movements. This robotic metamaterial is designed as a micro 3D lattice structure that integrates piezoelectric, conductive, and structural elements. It can undergo numerous deformation modes, including twisting, shear, normal deformation, and combinations and amplifications of these modes. Such robotic metamaterials surpass the limitations of natural piezoelectric crystals and are expected to directly influence the development of future micro-robots and transducers.[118]

3D printing of piezoelectric materials allows for the precise fabrication of complex shapes and structures, applicable in various fields such as energy harvesters and sensors. This technology enables the design of multifunctional sensors with integrated capabilities. In addition, 3D printing facilitates the structural optimization of lightweight actuators. However, products manufactured through this method may have reduced durability compared to those produced by traditional methods, and minor defects that occur during the printing process can lead to performance degradation. Consequently, further research and development are needed to enhance the piezoelectric efficiency and durability of these materials, addressing the challenges inherent in the 3D printing process to ensure reliable and robust performance in practical applications.

3.5. Thermoelectrics

Thermoelectrics directly transform the temperature difference into electric current and vice versa using the

Peltier and Seebeck effects. This feature can be utilized in various fields, such as energy harvesting, cooling systems, and sensors.[119] As the potential difference generated within a single p-n semiconductor remains at the millivolt scale, thermoelectric devices achieve higher voltages by linking multiple p-n semiconductors in series.[120] For the n-type component, cationic materials such as TiO_{2-x} and $BixSb_{2-x}Te_{3-y}$, while for the p-type component, anionic materials such as Ni and $Bi_2(SeyTe_{1-y})_3$ are used.

The inefficiency in utilizing thermal energy stems from the limitation of traditional thermoelectric device manufacturing, which is confined to a 2D plane. Therefore, 3D printing technology, which can overcome these limitations, is gaining attention. There are various thermoelectric manufacturing technologies utilizing the 3D printing method, including material jetting, vat photopolymerization, materials extrusion, PBF (SLS), screen printing, dispenser printing, and inkjet printing.[17,120-124] These techniques offer benefits, including the capability to create precise structures, reduce material wastage, apply diverse materials, and expedite the prototyping process.[119] Recent advances in 3D printing technology for thermoelectric materials are summarized in Table 6, highlighting their improved performance and applications in thermoelectric cooler and generator.

3.5.1. Thermoelectric coolers

Thermoelectric coolers (TECs), which function based on the Peltier effect, offer various advantages. TECs enable precise temperature control by directly adjusting power through variations in input current. Furthermore, they have the benefits of low noise and minimized size due to the absence of compressors.[125] Therefore, numerous studies have been conducted to enhance stability and increase cooling efficiency.

Li *et al.*[126] fabricated flexible thermoelectric thick films using screen printing on a polyimide substrate with a $Bi_{0.5}Sb_{1.5}Te_3$/epoxy composite. These films created a temperature difference from 4.2 to 7.8 K when the current was between 0.01 and 0.05 A, with a power factor (PF) of 1.12 mW/m·K^{-2}. This achievement expands the potential of the flexible TECs with better cooling performance based on the higher PF value. Lu *et al.*[127] utilized inkjet printing to fabricate thin film TECs using nanoparticle materials: p-type $Sb_{1.5}Bi_{0.5}Te_3$ size of 9.8 ±2.7 nm and n-type $Bi_2Te_{2.7}Se_{0.3}$ size of 7.6 ± 1.9 nm on a polyimide (PI) substrate. The maximum PF was approximately 77 μW/m·K^{-2} at 75°C. This finding suggests the potential for improving the drawbacks of conventional nanoparticle thin-film manufacturing processes, such as complex manufacturing processes and material wastage. Since thin films are superior in localizing cooling and heating compared to bulk devices,[128] they will lead to advancements in fields such as microelectronics and thermochemistry-on-a-chip.

3.5.2. Thermoelectric generators (TEGs)

The Seebeck effect is an electrical phenomenon observed between two semiconductors due to a temperature difference, where electrons migrate from one material to another in response to the temperature gradient. TEGs function based on the Seebeck effect, and they can generate electricity from small temperature differences, with the advantages of minimal size and lightweight. Therefore, numerous studies have been conducted to enhance stability and broaden the scalability of application areas. A state-of-the-art, flexible TEG with metal chalcogenide nanowires was developed through inkjet printing. The printed films achieved a PF of 493.8 μW/m·K^{-2} at 400 K and a power density of 0.9 μW/m·K^{-2} using materials such as Ag_2Te, Cu_7Te_4, and $Bi_2Te_{2.7}Se_{0.3}$.[129] This development enhanced both parameters and demonstrated promising scalability for novel materials. Moreover, a flexible TEG on a paper substrate was developed through dispenser printing. Materials such as $Bi_{0.5}Sb_{1.5}Te_3$ and $Bi_2Se_{0.3}Te_{2.7}$ were used, achieving an output power and voltage

Table 6. Comparison of materials and fabrication methods for thermoelectric

Printing Method	Composition	Application	Performance	Reference
Screen	Bi0.5Sb1.5Te3/epoxy composite	TEC	Temperature difference from 4.2 to 7.8 K with current 0.01 to 0.05 A, at PF of 1.12 mW/m·K^{-2}	126
Inkjet	p-type $Sb_{1.5}Bi_{0.5}Te_3$ n-type $Bi_2Te_{2.7}Se_{0.3}$	TEC	PF of 77 μW/m·K^{-2} at 75°C	127
Inkjet	Ag_2Te, Cu_7Te_4, $Bi_2Te_{2.7}Se_{0.3}$	TEG	PF of 493.8 μW/m·K^{-2} at 400 K and power density of 0.9 μW/m·K^{-2}	129
Dispenser	$Bi_{0.5}Sb_{1.5}Te_3$, Bi2$Se_{0.3}Te_{2.7}$	TEG	Output power and voltage of 10 nW and 8.3 mV, respectively, with a thousand bending cycles at 35K	124
Ink dispensing	SWCNTs/SDBS, SWCNTs/CTAB	TEG	PF values of 308 μW/m·K^{-2} and 258 μW/m·K^{-2} for the p-type and n-type film, respectively	130

Abbreviations: PF: Power factor; SWCNTs/CTAB: Single-walled carbon nanotubes/cetyltrimethylammonium bromide; SWCNTs/SDBS: Single-walled carbon nanotubes/sodium dodecylbenzene sulfonate; TEC: Thermoelectric cooler; TEG: Thermoelectric generator.

of 10 nW and 8.3 mV, respectively, after a thousand bending cycles at 35 K.[124] Figure 6B illustrates the manufacturing process and the complete structure of the flexible TEG. This research indicates the potential for printing TEGs on paper, which is widely used in various industries, thus enhancing the scalability of TEGs. Furthermore, Mytafides *et al.*[130] fabricated TEGs using ink dispensing with single-walled carbon nanotube (SWCNT) material. The resulting TEGs achieved high flexibility and PF values of 308 μW/m·K^{-2} and 258 μW/m·K^{-2} for the p-type and n-type film, respectively. The materials used were SWCNTs/sodium dodecylbenzene sulfonate and SWCNTs/cetyltrimethylammonium bromide. These TEGs maintained stability even in encapsulated conditions, demonstrating the potential for advancing TEG technology by adopting new materials and producing durable TEGs for applications in extreme conditions. Figure 6A depicts the structural composition, flexibility, and overall construction of the fabricated TEGs.

3.6. Carbon-based materials

Carbon-based materials are compounds consisting of carbon atoms, with properties varying according to their chemical structure. They generally exhibit lightweight, high strength, electrical and thermal conductivity, and chemical stability. Examples of carbon-based materials include graphene, which consists of widely spread carbon atoms, carbon nanotubes (CNTs) with a cylindrical structure, and fullerenes with a spherical shape. These materials find wide applications in various fields, such as microelectronics, electrochemical biosensors, strain sensors, and chemical sensors.[131,132] At present, the general manufacturing methods for carbon-based materials are chemical vapor deposition (CVD) and arc discharge. However, CVD has disadvantages, such as the use of numerous solvents, complex manufacturing processes, and high costs. The arc discharge method may also be susceptible to impurities and material wastage.[133] Therefore, various printing techniques such as DIW, binder jetting, inkjet printing, spray coating, FDM, and SLS have been developed to address these problems. These methods offer advantages such as simplification of processes, precise structure printing, minimal material wastage, and rapid prototyping. However, challenges remain, including high porosity, weak connections between layers, and ensuring the production of high-quality materials.[134] Recent advances in 3D printing technology for carbon-based materials are summarized in Table 7, with improved performance and applications in sensor and battery.

3.6.1. Carbon-based sensors

Carbon-based chemical and strain sensors have revolutionized modern sensing technology. Chemical

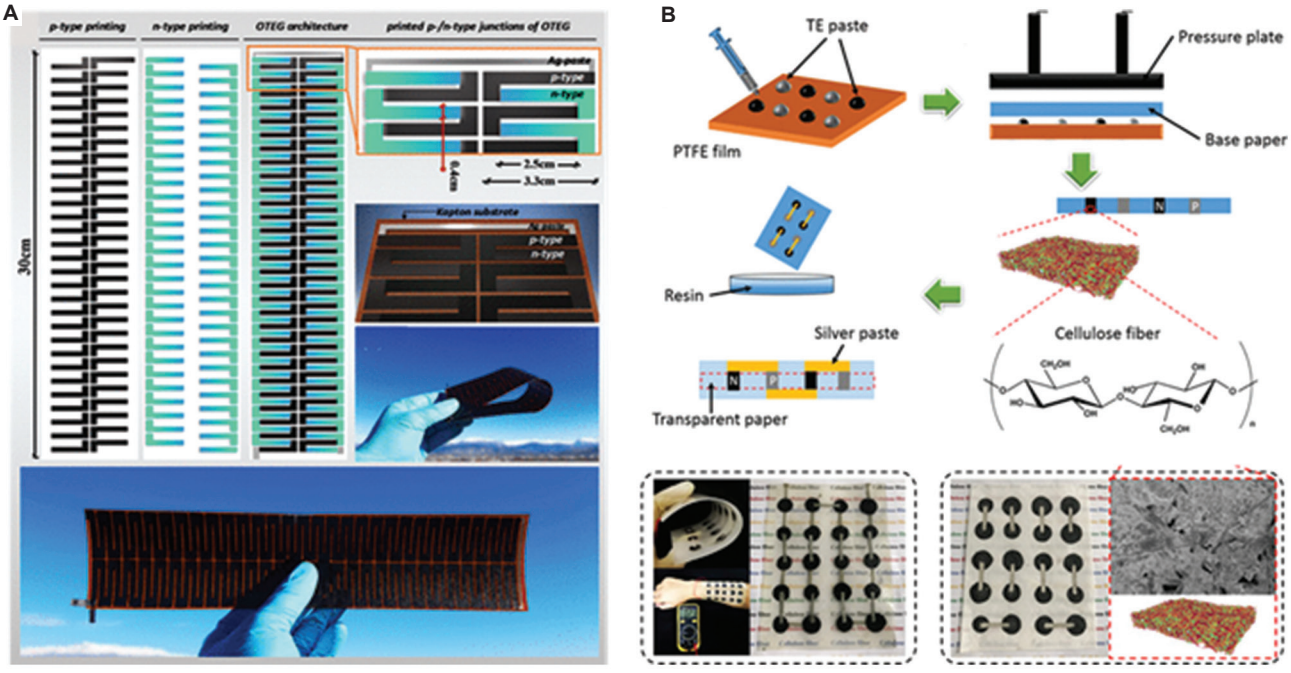

Figure 6. Applications of thermoelectric materials. (A) Fabrication of an all-carbon, fully printed, and flexible thermoelectric generator, including its structure, flexibility, and overall composition. Images reproduced with permission from Mytafides *et al.*[130] Copyright 2021 © American Chemical Society. (B) Schematic diagram illustrating the fabrication process and the resulting transparent paper-based flexible thermoelectric generator. Images reproduced with permission from Zhao *et al.*[124] Copyright © 2019 American Chemical Society. Abbreviations: OTEG: Organic thermoelectric generator; PTFE: Polytetrafluoroethylene; TE: Thermoelectric.

Table 7. Comparison of materials and fabrication methods for carbon-based materials

Printing method	Composition	Application	Performance	References
Inkjet	Poly (3,4ethylenedioxythiophene), COOH, PEDOT: PSS, CNT	Chemical sensor	Sensitivity (ΔS/ΔC) of 24.4×10^{-4} and short response/recovery times of 13/60 at 1000 ppm	135
Screen	Graphene-carbon ink	Humidity sensor	resistance-humidity gradient was~12.4 Ω/%RH (room humidity) on 25%RH to 91.7%RH	136
Extrusion	Pristine graphene formulated from ethyl cellulose, toluene/ethanol	VOC sensor	Detect chemical substances - ethanol, methanol, and acetone within the range of 5 to 100 ppm.	142
Laser-induced forward transfer	SWCNTs/SnO2 NPs	Chemical sensor (NH_3)	At room temperature, NH_3 response time of 13 s for 25 ppm	144
Meniscus	MWNTs, PVP	Strain sensor	Gauge factors of 12.87 at compressive strain and 13.07 at tensile strain at over 1500 bending cycles	137
FDM	Graphene-based polylactic acid, TPU	Strain sensor	High level of sensitivity	138
Inkjet	Graphene nano-sheets, green solvent: ethanol, stabilizer: 1 wt% ethyl-cellulose	Battery	~942 mAh/g at 0.1 C. With the 100 cycles of bending, 87% capacity remained.	140
Inkjet	$LiFePO_4$/AB/CNT	Battery	150 mAh/g at 0.1 C with 150 cycles	141
Vat photopolymerization (SLA)	PEGDA, Sudan I, GPE, PC, EC, Carbon black	Battery	Capacity of 1.4 μAh/cm^2 after 2 cycles.	143

Abbreviations: AB: Acetylene Black; CNT: Carbon nanotube; EC: Ethylene Carbonate; FDM: Fused deposition modeling; GPE: Gel Polymer Electrolyte; MWNTs: Multiwall nanotubes; NPs: Nanoparticles; PC: Propylene Carbonate; PEDOT: PSS: Poly (3,4-ethylenedioxythiophene) polystyrene sulfonate; PVP: Polyvinylpyrrolidone; SLA: Stereolithography; SWCNTs: Single-walled carbon nanotube; TPU: Thermoplastic polyurethane; VOC: Volatile organic compound.

sensors exhibit notable sensitivity to various compounds, with short response and recovery times. Similarly, strain sensors can sensitively detect structural deformations and stresses. Consequently, carbon-based chemical and strain sensors demonstrate innovative application potentials across various industries.

(a) Chemical sensors

Chemical sensors rely on chemical reactions altering the material's properties, forming the fundamental principle of their operation. Due to the durability and outstanding properties of carbon-based materials, they are often utilized in chemical sensors. For instance, a highly sensitive flexible ethanol sensor was developed using inkjet printing, functionalized with poly(3,4-ethylenedioxythiophene) and carboxylic acid (COOH) poly (styrenesulfonate) (PEDOT: PSS) CNT. It exhibits a sensitivity (ΔS/ΔC) of 24.4×10^{-4} and short response/recovery times of 13/60 at 1000 ppm.[135] Its high sensitivity is anticipated to lead to the development of precise ethanol sensors. In addition, a humidity sensor was developed using graphene-carbon ink through screen printing on substrates such as glossy paper, matt paper, and sylvicta. The sensor resistance-humidity gradient was approximately 12.4 Ω/%RH (room humidity) from 25% RH to 91.7% RH. It displayed flexibility, stability, repeatability, durability, and short response/recovery time.[136] Detecting humidity is essential across diverse industries, environmental monitoring, and health-care sectors, making it applicable in various fields. Furthermore, a volatile organic compound sensor was developed using pristine graphene formulated from ethyl cellulose and toluene/ethanol through extrusion printing.[137] Sized approximately 12 μm, it demonstrated the capability to detect chemical substances such as ethanol, methanol, and acetone within the range of 5 – 100 ppm. A formula relating concentration in ppm and resistance variation was derived, enabling current concentration measurements. The miniaturization of existing sensors suggests the potential to advance portable chemical sensor technology, thereby leading to the development of portable chemical sensors. Furthermore, Anca *et al.*[138] fabricated NH_3 detectable chemical sensors using laser-induced forward transfer printing. The minimum detectable NH_3 value was 25 ppm, with a response time of 13 s, showcasing an expansion of the manufacturing process.

(b) Strain sensors

The strain-sensitive property of an object, influenced by its structure, undergoes changes when subjected to mechanical forces such as tension or compression. This alteration in the property enables accurate measurement of strain experienced by the object.

Flexible strain sensors were developed using CNT ink with multiwall nanotubes and PVP through meniscus-guided printing based on the principle of piezoresistivity. This sensor achieved gauge factors of 12.87 at compressive strain and 13.07 at tensile strain and maintained its

performance over approximately 1500 bending cycles (Figure 7A and B).[139] This research, by enhancing the gauge factor, has improved precision and shown new potential in fields such as robotics engineering and wearable sensors, which demand precise measurements. In addition, a strain sensor using graphene-based polylactic acid with TPU was developed through FDM. It operates on the principle of piezoresistivity, calculating variations in resistance induced by applied tensile and compressive strain.[140] The study demonstrated the possibility of enhancing flexibility by more than fourfold while maintaining a high level of sensitivity comparable to that of a typical graphene sensor.

3.6.2. Batteries

Most lithium-ion batteries share similar shapes and solid properties. However, since the majority of electronic devices use batteries and their design must accommodate the battery, it hinders the free design of electric devices. To overcome these drawbacks, there is increasing attention on 3D printing technology, which enables free control of shapes and the fabrication of precise structures, including flexible batteries. Consequently, research is progressing on 3D printing carbon-based materials, which constitute the major parts of a battery, to address these problems.

A state-of-the-art flexible battery was developed with a CNT: MnO_2 anode. It achieved a capacity of 63 μAh cm^{-2} at 0.4 mA cm^{-2} and experienced only a 2.72% loss in capacity when the battery was bent.[141] This advancement holds promise for the development of wearable electronic devices, medical devices, and smart clothing. Furthermore, a lithium-ion battery utilizing graphene nanosheets with solvent exfoliation using green solvent (ethanol) and stabilizer (1 wt% ethyl-cellulose) was developed through inkjet printing. The battery achieved a capacity of approximately 942 mAh/g at 0.1 C. Even after 100 cycles of bending, the electrode retained approximately 87% of its initial capacity, as shown in Figure 7C.[142] It demonstrated outstanding battery performance and scalability in industries such as smartphones and automobiles. Furthermore, a lithium-ion

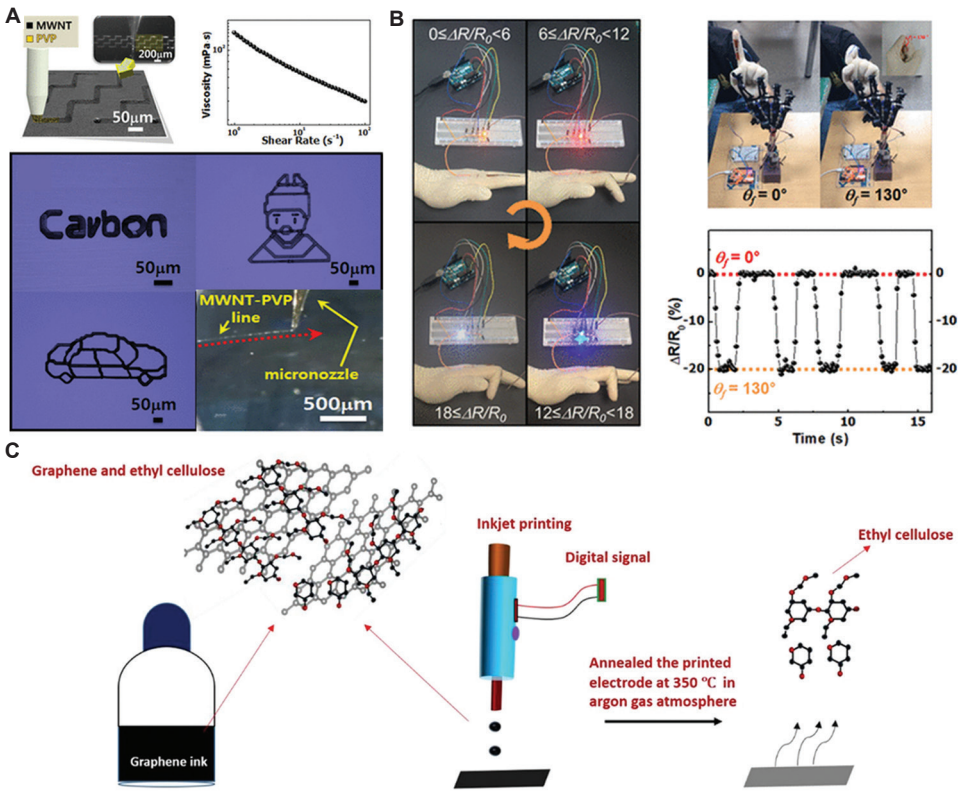

Figure 7. Fabrication and application of carbon-based materials. (A) Schematic diagram illustrating the meniscus-guided printing process for fabricating a transparent paper-based flexible thermoelectric generator (TEG), along with its resulting structure. (B) The fabrication process of an all-carbon fully printed and flexible TEG, including its structure, flexibility, and overall composition. Images in (A) and (B) reproduced with permission from Wajahat *et al.*[137] Copyright © 2018 American Chemical Society. (C) A schematic depiction of the graphene ink, inkjet-printing process, and annealing of printed samples in the production of graphene thin-film electrodes for use in lithium-ion batteries. Images reproduced with permission from Kushwaha *et al.*[142] Copyright © 2021 American Chemical Society.

battery using $LiFePO_4$/AB/CNT was developed through inkjet printing. It demonstrated a specific capacity of 150 mAh/g at 0.1 C with 150 cycles.[143] This study represents the fabrication of thick electrodes with high-power density and energy density, revealing the potential for high-performance energy storage devices. Furthermore, Chen *et al.*[144] developed a lithium-ion micro-battery using carbon black through SLA. The battery exhibited a capacity of 1.4 $\mu Ah/cm^2$ after two cycles of charging. This study signifies the expansion of existing manufacturing methods.

4. Conclusion and future perspectives

The promising and essential AM technology, pivotal for the Fourth Industrial Revolution, offers tremendous utility in manufacturing, spanning from product development to efficient production and small-batch manufacturing of diverse products. The advancement of AM technology has led to the development of materials with enhanced performance and novel characteristics, alongside the introduction of efficient and precise manufacturing systems to the market. Particularly, intensive research on functional materials based on polymer substrates and their applications is currently underway, showcasing their immense potential value.

In this review, we categorize the AM technologies primarily used for manufacturing functional polymer materials based on their manufacturing methods and operational principles. Subsequently, we examine the AM processes based on the characteristics of functional materials. By emphasizing the key features of each material, we support an upward approach to functional polymer design, enabling not only optimal process ability but also the achievement of multifunctional and complex shape manufacturing.

Next, we investigate the functional properties primarily utilized in current polymer-based functional materials. The development of functional materials based on polymers is predominantly focused on photosensitive resins. Extensive research has been conducted on the development of functional resins with properties such as biocompatibility, electrical conductivity, and magnetism. For instance, research on biocompatible resins is progressing for the optimal design of artificial organs and internal implants. In addition, research on functional materials for various applications, such as sensors, actuators, and soft robots, utilizing electrical conductivity and magnetism, is ongoing. Studies showcasing the achievement of special functionalities through the utilization of the unique 3D manufacturing capabilities and mixed production characteristics of AM technologies have also been examined.

Furthermore, we explore the development of functional components with various structures utilizing AM technologies, such as piezoelectric, thermoelectric, and perovskite materials. The advancement of functional components usable in diverse applications such as energy harvesting, displays, and sensors has been facilitated by the development of AM technologies. Integration with polymer materials has enabled manufacturing on curved surfaces, the development of flexible components, and the enhancement of functional properties, maximizing the utilization methods and fields of AM technologies.

This review emphasizes the importance of functional polymer materials in expanding the scope and capabilities of AM processes. Active participation in diversifying material options to meet the varied requirements of modern manufacturing, ranging from photosensitive resins to polymer powders, filaments, and viscous inks, is evident in recent research. Novel functional polymer materials with enhanced conductivity, actuation, and other functionalities hold huge potential across various application domains, from biocompatible implants to smart robots.

Overall, the rapid growth of research environments and technological advancements in polymer materials for AM signify a promising future where AM becomes an essential and complementary component of the modern manufacturing ecosystem. Through continuous interdisciplinary collaboration and innovation, the vision of realizing fully functional custom products through AM will be achieved.

Acknowledgments

None.

Funding

This work was supported by the Technology Development Program (Grant No. S3248116) funded by the Ministry of SMEs and Startups (MSS, Korea), and the National Research Foundation of Korea (NRF) grant under the Korea government (MSIT) (no. RS-2023-00211636).

Conflicts of interest

The authors declare that they have no competing interests.

Authors' contributions

Conceptualization: Im Doo Jung, Hayeol Kim
Investigation: All authors
Writing – original draft: All authors
Writing – review and *editing:* Im Doo Jung, Hayeol Kim

Ethics approval and consent to participate

Not applicable.

Consent for publication

Not applicable.

Availability of data

Not applicable.

References

1. Madhavadas V, Srivastava D, Chadha U, *et al*. A review on metal additive manufacturing for intricately shaped aerospace components. *CIRP J Manuf Sci Technol*. 2022;39:18-36.

   doi: 10.1016/j.cirpj.2022.07.005

2. Park JW, Shin YC, Kang HG, *et al*. *In vivo* analysis of post-joint-peserving surgery fracture of 3D-printed Ti-6Al-4V implant to treat bone cancer. *Bio Des Manuf*. 2021;4:879-888.

   doi: 10.1007/s42242-021-00147-2

3. Kim T, Kim JG, Park S, *et al*. Virtual surface morphology generation of Ti-6Al-4V directed energy deposition via conditional generative adversarial network. *Virtual Phys Prototyp*. 2023;18(1):e2124921.

   doi: 10.1080/17452759.2022.2124921

4. Tan LJ, Zhu W, Zhou K. Recent progress on polymer materials for additive manufacturing. *Adv Funct Mater*. 2020;30(43):2003062.

   doi: 10.1002/adfm.202003062

5. Wu H, Fahy WP, Kim S, *et al*. Recent developments in polymers/polymer nanocomposites for additive manufacturing. *Prog Mater Sci*. 2020;111:100638.

   doi: 10.1016/j.pmatsci.2020.100638

6. Li J, Lin X, Kang N, Lu J, Wang Q, Huang W. Microstructure, tensile and wear poperties of a novel graded al matrix composite pepared by direct energy deposition. *J Alloy Compd*. 2020;826:154077.

   doi: 10.1016/j.jallcom.2020.154077

7. Seo E, Sung H, Jeon H, *et al*. Laser powder bed fusion for AI assisted digital metal components. *Virtual Phys Prototyp*. 2022;17(4):806-820.

   doi: 10.1080/17452759.2022.2068804

8. Hotz H, Zimmermann M, Greco S, Kirsch B, Aurich JC. Additive manufacturing of functionally graded Ti-Al structures by laser-based direct energy deposition. *J Manuf Process*. 2021;68:1524-1534.

   doi: 10.1016/j.jmapro.2021.06.068

9. Jung ID, Lee MS, Lee J, *et al*. Embedding sensors using selective laser melting for self-cognitive metal parts. *Addit Manuf*. 2020;33:101151.

   doi: 10.1016/j.addma.2020.101151

10. Lee MS, Kim H, Koo YT, *et al*. Selective laser melting process for sensor embedding into SUS316L with heat dissipative inner cavity design. *Met Mater Int*. 2022;28:1-9.

    doi: 10.1007/s12540-021-01106-3

11. Lee J, Choe J, Park J, Yu JH, Kim S, Sung H. Microstructural effects on the tensile and fracture behavior of selective laser melted H13 tool steel under varying conditions. *Mater Charact*. 2019;55:109817.

    doi: 10.1016/j.matchar.2019.109817

12. Verma S, Yang CK, Lin CH, Jeng JY. Additive manufacturing of lattice structures for high strength mechanical interlocking of metal and resin during injection molding. *Addit Manuf*. 2022;49:102463.

    doi: 10.1016/j.addma.2021.102463

13. Joyee EB, Pan Y. Additive manufacturing of multi-material soft robot for on-demand drug delivery applications. *J Manuf Process*. 2020;56:1178-1184.

    doi: 10.1016/j.jmapro.2020.03.059

14. Rafiee M, Farahani RD, Therriault D. Multi-material 3D and 4D printing: A survey. *Adv Sci*. 2020;7(12):1902307.

    doi: 10.1002/advs.201902307

15. Champeau M, Heinze DA, Viana TN, de Souza ER, Chinellato AC, Titotto S. 4D printing of hydrogels: A review. *Adv Funct Mater*. 2020;30(31):1910606.

    doi: 10.1002/adfm.201910606

16. Liu J, Shang Y, Shao Z, Liu X, Zhang C. Three-dimensional printing to translate simulation to architecting for three-dimensional high performance piezoelectric Energy harvester. *Ind Eng Chem Res*. 2021;61(1):433-440.

    doi: 10.1021/acs.iecr.1c04433

17. Zhang D, Lim WYS, Duran SSF, Loh XJ, Suwardi A. Additive manufacturing of thermoelectrics: Emerging trends and outlook. *ACS Energy Lett*. 2022;7(2):720-735.

    doi: 10.1021/acsenergylett.1c02553

18. Park JW, Seo E, Park H, *et al*. Hybrid solid mesh structure for electron beam melting customized implant to treat bone cancer. *Int J Bioprinting*. 2023;9(4):716.

    doi: 10.18063/ijb.716

19. Culmone C, Smit G, Breedveld P. Additive manufacturing of medical instruments: A state-of-the-art review. *Addit Manuf*. 2019;27:461-473.

    doi: 10.1016/j.addma.2019.03.015

20. Huang J, Chen Q, Jiang H, *et al*. A survey of design methods for material extrusion polymer 3D printing. *Virtual Phys Prototyp*. 2020;15(2):148-162.

    doi: 10.1080/17452759.2019.1708027

21. Hossain SS, Gao B, Park S, Bae CJ. Incorporating nanoparticles in alumina ink for improved solid-loading

and sinterability of extrusion-based 3D printing. *ACS Appl Nano Mater*. 2022;5(12):17828-17838.

doi: 10.1021/acsanm.2c03792

22. Kim JH, Park S, Ahn J, *et al*. Meniscus-guided micro-printing of prussian blue for smart electrochromic display. *Adv Sci*. 2023;10(3):2205588.

doi: 10.1002/advs.202205588

23. Lee S, Kim JH, Wajahat M, *et al*. Three-dimensional printing of silver microarchitectures using newtonian nanoparticle inks. *ACS Appl Mater Interfaces*. 2017;9(22):18918-18924.

doi: 10.1021/acsami.7b02581

24. Gu X, Shaw L, Gu K, Toney MF, Bao Z. The meniscus-guided deposition of semiconducting polymers. *Nat Commun*. 2018;9(1):534.

doi: 10.1038/s41467-018-02833-9

25. Pagac M, Hajnys J, Ma QP, *et al*. A review of vat photopolymerization technology: Materials, applications, challenges, and future trends of 3D printing. *Polymers*. 2021;13(4):598.

doi: 10.3390/polym13040598

26. Gross B, Lockwood SY, Spence DM. Recent advances in analytical chemistry by 3D printing. *Anal Chem*. 2017;89(1):57-70.

doi: 10.1021/acs.analchem.6b04344

27. Chiappone A, Fantino E, Roppolo I, *et al*. 3D printed PEG-based hybrid nanocomposites obtained by sol-gel technique. *ACS Appl Mater Interfaces*. 2016;8(8):5627-5633.

doi: 10.1021/acsami.5b12578

28. Wang W, Liu S, Liu L, Alfarhan S, Jin K, Chen X. High-speed and high-resolution 3D printing of self-healing and ion-conductive hydrogels via μCLIP. *ACS Mater Lett*. 2023;5(6):1727-1737.

doi: 10.1021/acsmaterialslett.3c00439

29. Jose RR, Rodriguez MJ, Dixon TA, Omenetto F, Kaplan DL. Evolution of bioinks and additive manufacturing technologies for 3D bioprinting. *ACS Biomater Sci Eng*. 2016;2(10):1662-1678.

doi: 10.1021/acsbiomaterials.6b00088

30. Ouyang H, Li X, Lu X, Xia H. Selective laser sintering 4D printing of dynamic cross-linked polyurethane containing diels-alder bonds. *ACS Appl Polym Mater*. 2022;4(5):4035-4046.

doi: 10.1021/acsapm.2c00565

31. Sireesha M, Lee J, Kiran ASK, Babu VJ, Kee BBT, Ramakrishna S. A review on additive manufacturing and its way into the oil and gas industry. *RSC Adv*. 2018;8(40):22460-22468.

doi: 10.1039/C8RA03194K

32. Hines L, Petersen K, Lum GZ, Sitti M. Soft actuators for small-scale robotics. *Adv Mater*. 2017;29(13):1603483.

doi: 10.1002/adma.201603483

33. Ju Y, Hu R, Xie Y, *et al*. Reconfigurable magnetic soft robots with multimodal locomotion. *Nano Energy*. 2021;87:106169.

doi: 10.1016/j.nanoen.2021.106169

34. Kim Y, Zhao X. Magnetic soft materials and robots. *Chem Rev*. 2022;122(5):5317-5364.

doi: 10.1021/acs.chemrev.1c00481

35. Zhang C, Li X, Jiang L, *et al*. 3D pinting of functional magnetic materials: From design to applications. *Adv Funct Mater*. 2021;31(34):2102777.

doi: 10.1002/adfm.20210277

36. Zhao R, Kim Y, Chester SA, Sharma P, Zhao X. Mechanics of hard-magnetic soft materials. *J Mech Phys Solids*. 2019;124:244-263.

doi: 10.1016/j.jmps.2018.10.008

37. Lantean S, Barrera G, Pirri CF, *et al*. 3D printing of magnetoresponsive polymeric materials with tunable mechanical and magnetic properties by digital light processing. *Adv Mater Technol*. 2019;4(11):1900505.

doi: 10.1002/admt.201900505

38. Shasha C, Krishnan KM. Nonequilibrium dynamics of magnetic nanoparticles with applications in biomedicine. *Adv Mater*. 2021;33(23):1904131.

doi: 10.1002/adma.201904131

39. Xiao Y, Du J. Superparamagnetic nanoparticles for biomedical applications. *J Mater Chem B*. 2020;8(3):354-367.

doi: 10.1039/C9TB01955C

40. Ghazanfari MR, Kashefi M, Shams SF, Jaafari MR. Perspective of Fe3O4 nanoparticles role in biomedical applications. *Biochem Res Int*. 2016;2016:7840161.

doi: 10.1155/2016/7840161

41. Wajahat M, Kim JH, Kim JH, Jung ID, Pyo J, Seol SK. 4D printing of ultrastretchable magnetoactive soft material architectures for soft actuators. *ACS Appl Mater Interfaces*. 2023;15(51):59582-59591.

doi: 10.1021/acsami.3c12173

42. Wu S, Hamel CM, Ze Q, Yang F, Qi HJ, Zhao R. Evolutionary algorithm-guided voxel-encoding printing of functional hard-magnetic soft active materials. *Adv Intell Syst*. 2020;2(8):2000060.

doi: 10.1002/aisy.202000060

43. Ren Z, Hu W, Dong X, Sitti M. Multi-functional soft-bodied jellyfish-like swimming. *Nat Commun*. 2019;10(1):2703.

doi: 10.1038/s41467-019-10549-7

44. Kim Y, Yuk H, Zhao R, Chester SA, Zhao X. Printing ferromagnetic domains for untethered fast-transforming soft materials. *Nature*. 2018;558(7709):274-279.

doi: 10.1038/s41586-018-0185-0

45. Zhang Y, Wang Q, Yi S, *et al*. 4D printing of magnetoactive soft materials for on-demand magnetic aactuation transformation. *ACS Appl Mater Interfaces*. 2021;13(3):4174-4184.

doi: 10.1021/acsami.0c19280

46. Kim Y, Parada GA, Liu S, Zhao X. Ferromagnetic soft continuum robots. *Sci Robot*. 2019;4(33):eaax7329.

doi: 10.1126/scirobotics.aax7329

47. Zhang Y, Pan C, Liu P, *et al*. Coaxially printed magnetic mechanical electrical hybrid structures with actuation and sensing functionalities. *Nat Commun*. 2023;14(1):4428.

doi: 10.1038/s41467-023-40109-z

48. Hofmann M. 3D printing gets a boost and opportunities with polymer materials. *ACS Macro Lett*. 2014;3(4):295-397.

doi: 10.1021/mz4006556

49. Xu T, Zhang J, Salehizadeh M, Onaizah O, Diller E. Millimeter-scale flexible robots with programmable three-dimensional magnetization and motions. *Sci Robot*. 2019;4(29):eaav4494.

doi: 10.1126/scirobotics.aav4494

50. Shao G, Ware HOT, Huang J, Hai R, Li L, Sun C. 3D printed magnetically-actuating micro-gripper operates in air and water. *Addit Manuf*. 2021;38:101834.

doi: 10.1016/j.addma.2020.101834

51. Siripongpreda T, Hoven VP, Narupai B, Rodthongkum N. Emerging 3D printing based on polymers and nanomaterial additives: Enhancement of properties and potential applications. *Eur Polym J*. 2021;184:111806.

doi: 10.1016/j.eurpolymj.2022.111806

52. Tan HW, An J, Chua CK, Tran T. Metallic nanoparticle inks for 3D printing of electronics. *Adv Electron Mater*. 2019;5(5):1800831.

doi: 10.1002/aelm.201800831

53. Huang Q, Zhu Y. Printing conductive nanomaterials for flexible and stretchable electronics: A review of materials, processes, and applications. *Adv Mater Technol*. 2019;4(5):1800546.

doi: 10.1002/admt.201800546

54. Tan HW, Choong YYC, Kuo CN, Low HY, Chua CK. 3D printed electronics: Processes, materials and future trends. *Prog Mater Sci*. 2022;127:100945.

doi: 10.1016/j.pmatsci.2022.100945

55. Yang C, Gu H, Lin W, *et al*. Silver nanowires: From scalable synthesis to recyclable foldable electronics. *Adv Mater*. 2011;23(27):3052-3056.

doi: 10.1002/adma.201100530

56. Fu D, Yang R, Wang Y, Wang R, Hua F. Silver nanowire synthesis and applications in composites: Progress and prospects. *Adv Mater Technol*. 2022;7(11):2200027.

doi: 10.1002/admt.202200027

57. Kim J, Kim WS. Stretching silver: Printed metallic nano inks in stretchable conductor applications. *IEEE Nanotechnol Mag*. 2014,8(4):6-13.

doi: 10.1109/MNANO.2014.2355274

58. Jo H, Park JS, Lim HY, Lee GY. Laser sintered silver nanoparticles on the PDMS for a wearable strain sensor capable of detecting finger motion. *ACS Appl Nano Mater*. 2023;6(24):22998-23011.

doi: 10.1021/acsanm.3c04386

59. Lee GY, Kim MS, Min SH, *et al*. Highly sensitive solvent-free silver nanoparticle strain sensors with tunable sensitivity created using an aerodynamically focused nanoparticle printer. *ACS Appl Mater Interfaces*. 2019;11(29):26421-26432.

doi: 10.1021/acsami.9b00943

60. Jain PK, El-Sayed IH, El-Sayed MA. Au nanoparticles target cancer. *Nano Today*. 2007;2(1):18-29.

doi: 10.1016/S1748-0132(07)70016-6

61. Boisselier E, Astruc D. Gold nanoparticles in nanomedicine: Preparations, imaging, diagnostics, therapies and toxicity. *Chem Soc Rev*. 2009;6:1759-1782.

doi: 10.1039/B806051G

62. Dykman L, Khlebtsov N. Gold nanoparticles in biomedical applications: Recent advances and perspectives. *Chem Soc Rev*. 2012;41:2256-2282.

doi: 10.1039/C1CS15166E

63. Park BK, Kim D, Jeong S, Moon J, Kim JS. Direct writing of copper conductive patterns by ink-jet printing. *Thin Solid Films*. 2007;515(19):7706-7711.

doi: 10.1016/j.tsf.2006.11.142

64. Jeong S, Woo K, Kim D, *et al*. Controlling the thickness of the surface oxide layer on Cu nanoparticles for the fabrication of conductive structures by ink-jet printing. *Adv Funct Mater*. 2008;18(5):671-830.

doi: 10.1002/adfm.200700902

65. Kim YJ, Ryu CH, Park SH, Kim HS. The effect of poly (N-vinylpyrrolidone) molecular weight on flash light sintering of copper nanopaste. *Thin Solid Films*. 2014;570:114-122.

doi: 10.1016/j.tsf.2014.09.035

66. Dharmadasa R, Jha M, Amos DA, Druffel T. Room temperature synthesis of a copper ink for the intense pulsed light sintering of conductive copper films. *ACS Appl Mater Interfaces*. 2013;5(24):12773-13484.

doi: 10.1021/am404226e

67. Zhan P, Jia Y, Zhai W, *et al*. A fibrous flexible strain sensor

with Ag nanoparticles and carbon nanotubes for synergetic high sensitivity and large response range. *Compos A Appl Sci Manuf*. 2023;167:107431.

doi: 10.1016/j.compositesa.2023.107431

68. Aslanidis E, Skotadis E, Tsoukalas D. Resistive crack-based nanoparticle strain sensors with extreme sensitivity and adjustable gauge factor, made on flexible substrates. *Nanoscale*. 2021;13(5):3263-3274.

doi: 10.1039/d0nr07002e

69. Soe HM, Manaf AA, Matsuda A, Jaafar M. Development and fabrication of highly flexible, stretchable, and sensitive strain sensor for long durability based on silver nanoparticles-polydimethylsiloxane composite. *J Mater Sci Mater Electron*. 2020;31:11897-11910.

doi: 10.1007/s10854-020-03744-6

70. Hammock ML, Chortos A, Tee BCK, Tok JBH, Bao Z. 25th Anniversary article: The evolution of electronic skin (E-Skin): A brief history, design considerations, and recent progress. *Adv Mater*. 2013;25(42):5997-6038.

doi: 10.1002/adma.201302240

71. Guo SZ, Qiu K, Meng F, Park SH, McAlpine MC. 3D printed stretchable tactile sensors. *Adv Mater*. 2017;29(27):1701218.

doi: 10.1002/adma.201701218

72. Valentine AD, Busbee TA, Boley JW, *et al*. Hybrid 3D printing of soft electronics. *Adv Mater*. 2017;29(40):1703817.

doi: 10.1002/adma.201703817

73. Zhu Z, Guo SZ, Hirdler T, *et al*. 3D printed functional and biological materials on moving freeform surfaces. *Adv Mater*. 2018;30(23):1707495.

doi: 10.1002/adma.201707495

74. Zhou LY, Gao Q, Zhan JF, Xie CQ, Fu JZ, He Y. Three-dimensional printed wearable sensors with liquid metals for detecting the pose of snakelike soft robots. *ACS Appl Mater Interfaces*. 2018;10(27):23208-23217.

doi: 10.1021/acsami.8b06903

75. Peng X, Kuang X, Roach DJ, *et al*. Integrating digital light processing with direct ink writing for hybrid 3D printing of functional structures and devices. *Addit Manuf*. 2021;40:101911.

doi: 10.1016/j.addma.2021.101911

76. Park NG. Perovskite solar cells: An emerging photovoltaic technology. *Mater Today*. 2015;18(2):65-72.

doi: 10.1016/j.mattod.2014.07.007

77. Zhang X, Turiansky ME, Shen JX, Van de Walle CG. Defect tolerance in halide perovskites: A first-principles perspective. *J Appl Phys*. 2022;131(9):090901.

doi: 10.1063/5.0083686

78. Motta C, El-Mellouhi F, Sanvito S. Charge carrier mobility in hybrid halide perovskites. *Sci Rep*. 2015;5(1):12746.

doi: 10.1038/srep12746

79. Wei Z, Chen H, Yan K, Yang S. Inkjet printing and instant chemical transformation of a CH3NH3PbI3/nanocarbon electrode and interface for planar perovskite solar cells. *Angew Chem Int Ed Engl*. 2014;53(48):13239-13243.

doi: 10.1002/anie.201408638

80. Mathies F, Abzieher T, Hochstuhl A, *et al*. Multipass inkjet printed planar methylammonium lead iodide perovskite solar cells. *J Mater Chem A*. 2016;4(48):19207-19213.

doi: 10.1039/c6ta07972e

81. Choi JW, Woo HC, Huang X, *et al*. Organic-inorganic hybrid perovskite quantum dots with high PLQY and enhanced carrier mobility through crystallinity control by solvent engineering and solid-state ligand exchange. *Nanoscale*. 2018;10(28):13356-13367.

doi: 10.1039/c8nr00806j

82. Liang H, Yuan F, Johnston A, *et al*. High color purity lead-free perovskite light-emitting diodes via sn stabilization. *Adv Sci* (*Weinh*). 2020;7(8):1903213.

doi: 10.1002/advs.201903213

83. Bak T, Kim K, Seo E, *et al*. Accelerated design of high-efficiency lead-free tin perovskite solar cells via machine learning. *Int J Precis Eng Manuf Green Technol*. 2023;10(1):109-121.

doi: 10.1007/s40684-022-00417-z

84. Ahmed T, Seth S, Samanta A. Boosting the photoluminescence of CsPbX3 (X=Cl, Br, I) perovskite nanocrystals covering a wide wavelength range by postsynthetic treatment with tetrafluoroborate salts. *Chem Mat*. 2018;30(11):3633-3637.

doi: 10.1021/acs.chemmater.8b01235

85. Li F, Liu SF, Liu W, *et al*. 3D printing of inorganic nanomaterials by photochemically bonding colloidal nanocrystals. *Science*. 2023;381(6665):1468-1474.

doi: 10.1126/science.adg6681

86. Liu J, Shabbir B, Wang C, *et al*. Flexible, printable soft-X-ray detectors based on all-inorganic perovskite quantum dots. *Adv Mater*. 2019;31(30):1901644.

doi: 10.1002/adma.201901644

87. Zheng J, Zhang M, Lau CFJ, *et al*. Spin-coating free fabrication for highly efficient perovskite solar cells. *Sol Energy Mater Sol Cells*. 2017;168:165-171.

doi: 10.1016/j.solmat.2017.04.029

88. Bishop JE, Smith JA, Lidzey DG. Development of spray-coated perovskite solar cells. *ACS Appl Mater Interfaces*. 2020;12(43):48237-48245.

doi: 10.1021/acsami.0c14540

89. Kim JH, Williams ST, Cho N, Chueh CC, Jen AKY. Enhanced environmental stability of planar heterojunction perovskite solar cells based on blade-coating. *Adv Energy Mater*. 2014;5(4):1401229.

doi: 10.1002/aenm.201401229

90. Zhang L, Chen S, Wang X, *et al*. Ambient inkjet-printed high-efficiency perovskite solar cells: Manipulating the spreading and crystallization behaviors of picoliter perovskite droplets. *Sol RRL*. 2021;5(5):2100106.

doi: 10.1002/solr.202100106

91. Chen M, Zhou Z, Hu S, *et al*. 3D printing of arbitrary perovskite nanowire heterostructures. *Adv Funct Mater*. 2023;33(15):2212146.

doi: 10.1002/adfm.202212146

92. Zhu M, Duan Y, Liu N, *et al*. Electrohydrodynamically printed high-resolution full-color hybrid perovskites. *Adv Funct Mater*. 2019;29(35):1903294.

doi: 10.1002/adfm.201903294

93. Tang Y, Liu B, Yuan H, *et al*. *In situ* synthesis of MAPbX3 perovskite quantum dot-polycaprolactone composites for fluorescent 3D printing filament. *J Alloy Compd*. 2022;916:164961.

doi: 10.1016/j.jallcom.2022.164961

94. Jeon H, Wajahat M, Park S, *et al*. 3D Printing of luminescent perovskite quantum dot-polymer architectures. *Adv Funct Mater*. 2024;2024:2400594.

doi: 10.1002/adfm.202400594

95. Eggers H, Schackmar F, Abzieher T, *et al*. Inkjet-printed micrometer-thick perovskite solar cells with large columnar grains. *Adv Energy Mater*. 2019;10(6):1903184.

doi: 10.1002/aenm.201903184

96. Wang Q, Zhang G, Zhang H, Duan Y, Yin Z, Huang Y. High-resolution, flexible, and full-color perovskite image photodetector via electrohydrodynamic printing of ionic-liquid-based ink. *Adv Funct Mater*. 2021;31(28):2100857.

doi: 10.1002/adfm.202100857

97. Satake K, Sato Y, Narazaki K, *et al*. Fabrication of perovskite nanocrystal light-emitting diodes via inkjet printing with high-temperature annealing. *ACS Appl Opti Mater*. 2022;1(1):282-288.

doi: 10.1021/acsaom.2c00053

98. Liu H, Shi G, Khan R, *et al*. Large-area flexible perovskite light-emitting diodes enabled by inkjet printing. *Adv Mater*. 2024;36(8):2309921.

doi: 10.1002/adma.202309921

99. Liu Y, Li F, Qiu L, *et al*. Fluorescent Microarrays of in situ crystallized perovskite nanocomposites fabricated for patterned applications by using inkjet printing. *ACS Nano*. 2019;13(2):2042-2049.

doi: 10.1021/acsnano.8b08582

100. Yang Z, Zhou S, Zu J, Inman D. High-performance piezoelectric energy harvesters and their applications. *Joule*. 2018;2(4):642-697.

doi: 10.1016/j.joule.2018.03.011

101. Wu Y, Ma Y, Zheng H, Ramakrishna S. Piezoelectric materials for flexible and wearable electronics: A review. *Mater Des*. 2021;211:110164.

doi: 10.1016/j.matdes.2021.110164

102. Smith GL, Pulskamp JS, Sanchez LM, *et al*. PZT-based piezoelectric MEMS technology. *J Am Ceram Soc*. 2012;95(6):1777-1792.

doi: 10.1111/j.1551-2916.2012.05155.x

103. Park KI, Xu S, Liu Y, *et al*. Piezoelectric BaTiO(3) thin film nanogenerator on plastic substrates. *Nano Lett*. 2010;10(12):4939-4943.

doi: 10.1021/nl102959k

104. Ueberschlag P. PVDF piezoelectric polymer. *Sens Rev*. 2001;21(2):118-126.

doi: 10.1108/02602280110388315

105. Bhavanasi V, Kumar V, Parida K, Wang J, Lee PS. Enhanced piezoelectric energy harvesting performance of flexible PVDF-TrFE bilayer films with graphene oxide. *ACS Appl Mater Interfaces*. 2016;8(1):521-529.

doi: 10.1021/acsami.5b09502

106. Zhilun G, Longtu L, Suhua G, Xiaowen Z. Low-temperature sintering of lead-based piezoelectric ceramics. *J Am Ceram Soc*. 1989;72(3):486-491.

doi: 10.1111/j.1151-2916.1989.tb06160.x

107. Wang H, Godara M, Chen Z, Xie H. A one-step residue-free wet etching process of ceramic PZT for piezoelectric transducers. *Sens Actuator A Phys*. 2019;290:130-136.

doi: 10.1016/j.sna.2019.03.028

108. Amagata Y, Mihara S, Nishioki N, Higuchi T. *A New Fabrication Method for Microactuators with Piezoelectric Thin Film Using Precision Cutting Technique*. United States: IEEE; 1996. p. 307-311.

doi: 10.1109/MEMSYS.1996.493999

109. Megdich A, Habibi M, Laperrière L. A review on 3D printed piezoelectric energy harvesters: Materials, 3D printing techniques, and applications. *Mater Today Commun*. 2023;35:105541.

doi: 10.1016/j.mtcomm.2023.105541

110. Zhang J, Ye S, Liu H, *et al*. 3D printed piezoelectric BNNTs nanocomposites with tunable interface and microarchitectures for self-powered conformal sensors. *Nano Energy*. 2020;77:105300.

doi: 10.1016/j.nanoen.2020.105300

111. Song L, Dai R, Li Y, Wang Q, Zhang C. Polyvinylidene fluoride energy harvester with boosting piezoelectric performance through 3D printed biomimetic bone structures. *ACS Sustain Chem Eng*. 2021;9(22):7561-7568.

doi: 10.1021/acssuschemeng.1c01305

112. Malakooti MH, Julé F, Sodano HA. Printed nanocomposite energy harvesters with controlled alignment of barium titanate nanowires. *ACS Appl Mater Interfaces*. 2018;10(44):38359-38367.

doi: 10.1021/acsami.8b13643

113. Liu CL, Du Q, Zhang C, Wu JM, Zhang G, Shi YS. Fabrication and properties of BaTiO3 ceramics via digital light processing for piezoelectric energy harvesters. *Addit Manuf*. 2022;56:102940.

doi: 10.1016/j.addma.2022.102940

114. Pabst O, Perelaer J, Beckert E, Schubert US, Eberhardt R, Tünnermann A. All inkjet-printed piezoelectric polymer actuators: Characterization and applications for micropumps in lab-on-a-chip systems. *Org Electron*. 2013;14(12):3423-3429.

doi: 10.1016/j.orgel.2013.09.009

115. Maity K, Mondal A, Saha MC. Cellulose nanocrystal-based all-3D-printed pyro-piezoelectric nanogenerator for hybrid energy harvesting and self-powered cardiorespiratory monitoring toward the human-machine interface. *ACS Appl Mater Interfaces*. 2023;15(11):13956-13970.

doi: 10.1021/acsami.2c21680

116. Islam MN, Rupom RH, Adhikari PR, *et al*. Boosting piezoelectricity by 3D printing PVDF-MoS2 composite as a conformal and high-sensitivity piezoelectric sensor. *Adv Funct Mater*. 2023;33(42):2302946.

doi: 10.1002/adfm.202302946

117. Nassar H, Khandelwal G, Chirila R, *et al*. Fully 3D printed piezoelectric pressure sensor for dynamic tactile sensing. *Addit Manuf*. 2023;71:103601.

doi: 10.1016/j.addma.2023.103601

118. Cui H, Yao D, Hensleigh R, *et al*. Design and printing of proprioceptive three-dimensional architected robotic metamaterials. *Science*. 2022;376(6599):1287-1293.

doi: 10.1126/science.abn0090

119. Burton M, Howells G, Atoyo J, Carnie M. Printed thermoelectrics. *Adv Mater*. 2022;34(18):e2108183.

doi: 10.1002/adma.202108183

120. Lee H, Chidambaram Seshadri R, Han SJ, Sampath S. TiO 2-X based thermoelectric generators enabled by additive and layered manufacturing. *Appl Energy*. 2017;192:24-32.

doi: 10.1016/j.apenergy.2017.02.001

121. Shin S, Kumar R, Roh JW, *et al*. High-performance screen-printed thermoelectric films on fabrics. *Sci Rep*. 2017;7(1):7317.

doi: 10.1038/s41598-017-07654-2

122. Juntunen T, Jussila H, Ruoho M, *et al*. Inkjet printed large-area flexible few-layer graphene thermoelectrics. *Adv Funct Mater*. 2018;28(22):1800480.

doi: 10.1002/adfm.201800480

123. Bulman G, Barletta P, Lewis J, *et al*. Superlattice-bsed thin-film thermoelectric modules with high cooling fluxes. *Nat Commun*. 2016;7:10302.

doi: 10.1038/ncomms10302

124. Zhao X, Han W, Zhao C, *et al*. Fabrication of transparent paper-based flexible thermoelectric generator for wearable energy harvester using modified distributor printing technology. *ACS Appl Mater Interfaces*. 2019;11(10):10301-10309.

doi: 10.1021/acsami.8b21716

125. Liu H, Li G, Zhao X, Ma X, Shen C. Investigation of the impact of the thermoelectric geometry on the cooling performance and thermal-mechanic characteristics in a thermoelectric cooler. *Energy*. 2023;267:126471.

doi: 10.1016/j.energy.2022.126471

126. Li P, Nie XL, Fang WB, *et al*. Fabrication and planar cooling performance of flexible Bi0.5Sb1.5Te3/epoxy composite thermoelectric films. *J Inorg Mater*. 2019;34(6):679.

doi: 10.15541/jim20180528

127. Lu Z, Layani M, Zhao X, *et al*. Fabrication of flexible thermoelectric thin film devices by inkjet printing. *Small*. 2014;10(17):3551-3554.

doi: 10.1002/smll.201303126

128. Venkatasubramanin R, Siivola E, Colpitts T, O'Quinn B. Thin-film thermoelectric devices with high room-temperature figures of merit. *Nature*. 2001;413:597-602.

doi: 10.1038/35098012

129. Du J, Zhang B, Jiang M, *et al*. Inkjet printing flexible thermoelectric devices using metal chalcogenide nanowires. *Adv Funct Mater*. 2023;33(26):2213564.

doi: 10.1002/adfm.202213564

130. Mytafides CK, Tzounis L, Karalis G, Formanek P, Paipetis AS. High-power all-carbon fully printed and wearable SWCNT-based organic thermoelectric generator. *ACS Appl Mater Interfaces*. 2021;13(9):11151-11165.

doi: 10.1021/acsami.1c00414

131. Schroeder V, Savagatrup S, He M, Lin S, Swager TM. Carbon nanotube chemical sensors. *Chem Rev*. 2019;119(1):599-663.

doi: 10.1021/acs.chemrev.8b00340

132. Jung ID, Kim M, Gao C, *et al*. Selective ion sweeping on prussian blue analogue nanoparticles and activated carbon

for electrochemical kinetic energy harvesting. *Nano Letters*. 2020;20(3):1800-1807.

doi: 10.1021/acs.nanolett.9b05029

133. Sidhu JS, Misra A, Bhardwaj A. Fabrication of Carbon Nanotube Components Using 3D Printing: Review. In: *Mater Today Proceedings*; 2023.

doi: 10.1016/j.matpr.2023.08.040

134. Lawes S, Riese A, Sun Q, Cheng N, Sun X. Printing nanostructured carbon for energy storage and conversion applications. *Carbon*. 2015;92:150-176.

doi: 10.1016/j.carbon.2015.04.008

135. Alshammari AS, Alenezi MR, Lai KT, Silva SRP. Inkjet printing of polymer functionalized CNT gas sensor with enhanced sensing properties. *Mater Lett*. 2017;189:299-302.

doi: 10.1016/j.matlet.2016.11.033

136. Beniwal A, Ganguly P, Aliyana AK, Khandelwal G, Dahiya R. Screen-printed graphene-carbon ink based disposable humidity sensor with wireless communication. *Sens Actuators B Chem*. 2023;374:132731.

doi: 10.1016/j.snb.2022.132731

137. Hassan K, Tung TT, Stanley N, *et al*. Graphene ink for 3D extrusion micro printing of chemo-resistive sensing devices for volatile organic compound detection. *Nanoscale*. 2021;13(10):5356-5368.

doi: 10.1039/d1nr00150g

138. Anca FB, Filipescu M, Voicu SI, Lippert T, Palla-Papavlu A. Facile fabrication of hybrid carbon nanotube sensors by laser direct transfer. *Nanomaterials* (*Basel*). 2021;11(10):2604.

doi: 10.3390/nano11102604

139. Wajahat M, Lee S, Kim JH, *et al*. Flexible strain sensors fabricated by meniscus-guided printing of carbon nanotube-polymer composites. *ACS Appl Mater Interfaces*. 2018;10(23):19999-20005.

doi: 10.1021/acsami.8b04073

140. Alsharari M, Chen B, Shu W. 3D printing of highly stretchable and sensitive strain sensors using graphene based composites. *Proceedings*. 2018;2:792.

doi: 10.3390/proceedings2130792

141. Ren Y, Meng F, Zhang S, *et al*. CNT@MnO2 composite ink toward a flexible 3D printed micro-zinc-ion battery. *Carbon Energy*. 2022;4(3):446-457.

doi: 10.1002/cey2.177

142. Kushwaha A, Jangid MK, Bhatt BB, Mukhopadhyay A, Gupta D. Inkjet-printed environmentally friendly graphene film for application as a high-performance anode in Li-Ion batteries. *ACS Appl Energy Mater*. 2021;4(8):7911-7921.

doi: 10.1021/acsaem.1c01249

143. Wang J, Sun Q, Gao X, *et al*. Toward high areal energy and power density electrode for Li-Ion batteries via optimized 3D printing approach. *ACS Appl Mater Interfaces*. 2018;10(46):39794-39801.

doi: 10.1021/acsami.8b14797

144. Chen Q, Xu R, He Z, Zhao K, Pan L. Printing 3D gel polymer electrolyte in lithium-ion microbattery using stereolithography. *J Electrochem Soc*. 2017;164:X18.

doi: 10.1149/2.0651709jes